Hyaluronan deposition in islets may precede and direct the location of islet immune cell infiltrates

DOI:
10.1007/s00125-019-05066-7

Document Version
Accepted author manuscript

Hyaluronan deposition in islets may precede and direct the location of islet immune cell infiltrates

Marika Bogdani[1*], Cate Speake[2], Mathew J. Dufort[3], Pamela Y. Johnson[1], Megan J. Larmore[4], Anthony J. Day[5], Thomas N. Wight[1], Åke Lernmark[6†], and Carla J. Greenbaum[2]

[1]Matrix Biology Program, Benaroya Research Institute at Virginia Mason, Seattle, WA, USA
[2]Diabetes Research Program and Clinical Research Center, Benaroya Research Institute at Virginia Mason, Seattle, WA, USA
[3]Bioinformatics department, Benaroya Research Institute at Virginia Mason, Seattle, WA, USA
[4]Histology and Imaging Core, University of Washington, Seattle, WA, USA
[5]Wellcome Trust Centre for Cell-Matrix Research, University of Manchester, Manchester, UK
[6]Department of Medicine, University of Washington, Seattle, WA

***Address correspondence to:**
Marika Bogdani MD, PhD
Matrix Biology Program
Benaroya Research Institute at Virginia Mason
1201 9th Avenue
Seattle, WA 98101, USA
Phone: 206.342.6994
E-mail: mbogdani@benaroyarsearch.org

ORCID iD: 0000-0002-4677-7523

[†]Å.L.'s present address is:
Department of Clinical Sciences, Lund University/CRC, Skåne University Hospital, SE-20502 Malmö, Sweden

Word number: 3961

Tweet
#Hyaluronan deposition in #pancreatic islets may precede and direct the location of islet immune cell infiltrates. Novel findings from @BRIautoimmune #type1diabetes #autoantibodies @ExtracellMatrix #insulitis @PancreaticCell

Abstract

Aims/hypothesis Substantial deposition of the extracellular matrix component hyaluronan (HA) is characteristic of insulitis in overt type 1 diabetes. We investigated whether HA accumulation is detectable in islets early in disease pathogenesis and how this affects the development of insulitis and the beta cell mass.

Methods Pancreas tissues from 15 non-diabetic organ donors positive for islet autoantibodies (aAbs) and from 14 age-matched aAb-negative controls were examined for the amount of islet HA staining and the presence of insulitis. The kinetics of HA deposition in islets along with the onset and progression of insulitis, and changes in beta cell mass were investigated in BioBreeding $DR^{lyp/lyp}$ rats (a model of spontaneous autoimmune diabetes) from 40 days of age until diabetes onset.

Results Abundant islet HA deposits were observed in pancreas tissues from 3 single and 4 double aAb+ donors (aAb+HA^{high}). In these 7 tissues, the islet HA-stained areas measured 1000±650 μm^2 and were 4-fold larger than those from aAb- controls. The aAb+HA^{high} tissues also showed a greater prevalence of islets highly rich in HA (17% of the islets contained largest HA-stained areas of >2000 μm^2 vs. less than 1% in the controls). The amount of islet HA staining was associated with the number of aAbs but not with the Human Leukocyte Antigen (HLA) genotype or changes in beta cell mass. Among the 7 aAb+HA^{high} tissues, 3 from single and one from double aAb+ donors did not show any islet immune cell infiltrates, indicating that HA accumulates in aAb+ donors independently of insulitis. The 3 aAb+HA^{high} tissues exhibiting insulitis had the largest HA-stained areas, and the islet infiltrating immune cells co-localized with the most prominent HA deposits (>2000 μm^2). Accumulation of HA in islets was evident prior to insulitis in 7-8-week-old pre-symptomatic $DR^{lyp/lyp}$ rats, in which islet HA-stained areas measured 2370±170 μm^2 and were 3-fold larger than in 6-week-old rats. This initial islet HA deposition was not concurrent with beta cell loss. Insulitis was first detected in 9-10-week-old rats in which the HA-stained areas were 4980±500 μm^2. At this age, the rats also exhibited a 40% reduction in beta cell mass. Further

enlargement of the HA-positive areas, measuring 7220±1300 μm^2, was associated with invasive insulitis. HA deposits remained abundant in islets of rats with destructive insulitis, which had lost 85% of their beta cells.

Conclusions/interpretation This study indicates that HA deposition in islets occurs early in type 1 diabetes and prior to insulitis, and points to a potential role of HA in triggering islet immune cell infiltration and promotion of insulitis.

Keywords: islet, autoantibodies, T1D, hyaluronan, extracellular matrix, insulitis

Abbreviations

aAb	Autoantibody
BB	Bio Breeding
DORmO	DO11.10xRIP-OVA
HA	Hyaluronan
ECM	Extracellular matrix
HLA	Human Leukocyte Antigen
LCA	Leukocyte common antigen
SYN	Synaptophysin

Research in context

What is already known about this subject?

- We previously reported that an extracellular matrix rich in HA is a prominent feature of insulitis in type 1 diabetes.
- Reducing the amount of islet HA using an inhibitor of HA synthesis attenuated insulitis in DORmO mice.

What is the key question?

- Does the accumulation of HA take place early in type 1 diabetes and prior to insulitis?

What are the new findings?

- Large HA deposits are present in islets in a subset of aAb+ organ donors and are the sites where the immune cells infiltrate the islets. The abundance of these deposits is associated with the number of aAb but not with the HLA genotype.
- Islet HA deposits form both in pancreata in which insulitis is not detected and in the immune cell-free islets in pancreata that exhibit insulitis, which indicates that islet immune cell infiltrates are not required for the initial islet HA deposition.
- Incipient HA accumulation precedes islet immune cell infiltration in presymptomatic $DR^{lyp/lyp}$ rats. Continual amassment of HA is associated with the appearance of the insulitic cells, and positively correlates with the degree of insulitis.

How might this impact on clinical practice in the foreseeable future?

- Our findings implicate accumulation of HA as a marker of early disease and as a mediator driving immune cell migration into islets, which opens the door for potential novel therapeutic interventions that target HA accumulation.

Introduction

The process of beta cell damage in type 1 diabetes starts long before the disease becomes overt and is influenced by both genetic and environmental factors [1, 2]. The early stage of disease pathogenesis is characterized by islet autoimmunity, marked by two or more of the four as yet identified type 1 diabetes - associated islet autoantibodies (aAbs) against insulin, GAD65, IA-2, or ZnT8, followed by increasing beta cell dysfunction and death, and then clinically apparent disease [1, 3-8]. A histopathologic hallmark of diabetes at the time of clinical onset is insulitis, an inflammatory cell infiltrate indicating an ongoing immune-cell mediated process in islets which presumptively results in beta cell destruction [9-15]. At present, what guides immune cell trafficking from the blood into islets is not known. Moreover, the initial changes in human islets which trigger the recruitment of immune cells have not been defined.

We have proposed that an increase in the amount of hyaluronan (HA), a major component of the islet extracellular matrix (ECM), takes place early in the natural course of type 1 diabetes and that HA accumulation promotes islet invasion by immune cells and functional impairment of beta cells [16, 17]. HA, a linear high molecular weight polysaccharide, amasses at sites of inflammation and has become recognized as a regulator of several aspects of inflammation, including leukocyte migration, angiogenesis, and generation of inflammatory cytokines [18-20]. Our previous observations of abundant HA in insulin-deficient islets and insulitis regions in type 1 diabetes establish a link between HA accumulation in islets, beta cell loss, and insulitis [16]. However, this association is based on islet changes resulting from a chronic process that has been ongoing for months to years. Whether islet HA accumulation is an early event in type 1 diabetes pathogenesis and how it influences the development of insulitis is not known. To address this question, we investigated the occurrence and distribution of islet HA deposits in the presence or absence of insulitis in pancreas tissues from non-diabetic aAb-positive (aAb+) organ donors. In addition, we evaluated the kinetics of HA accumulation in islets concurrently with the extent of islet

immune cell infiltration and changes in beta cell mass in presymptomatic BB $DR^{lyp/lyp}$ rats during the progression to hyperglycemia.

Methods

Donors and tissue procurement Pancreas tissues samples from non-diabetic organ donors were obtained through the Network for Pancreatic Organ Donors with Diabetes. Samples were from 10 single aAb+, 5 double aAb+, and 14 age-matched control aAb-negative (aAb-) donors. Clinical characteristics of the donors are shown in ESM Table 1. For each donor, we randomly sampled six paraffin blocks from different regions of the pancreas. The pancreas tissues are referred to henceforth as "tissues". All the experiments were carried out with the approval of the Institutional Review Board of the Benaroya Research Institute (BRI).

BB DR/Rhw rats The BB rat model of autoimmune diabetes shares characteristics common to human disease including spontaneous hyperglycemia, ketoacidosis, genetic susceptibility, and insulitis [21]. Male and female BB $DR^{+/+}$, $DR^{lyp/+}$, and $DR^{lyp/lyp}$ rats [22] were housed in a specific-pathogen-free facility at the University of Washington on a 12-hour light/dark cycle and were fed a regular diet (Harlan Teklad, Madison, WI) and water *ad libitum*. Diabetes develops spontaneously by 12 weeks of age in $DR^{lyp/lyp}$ rats, while the diabetes-resistant ($DR^{+/+}$ and $DR^{lyp/+}$) rats remain diabetes-free throughout life [22, 23]. The colony was maintained by intercrossing $DR^{lyp/+}$ rats. These crosses generated $DR^{lyp/lyp}$ rats as well as $DR^{lyp/+}$ and $DR^{+/+}$ controls. The $DR^{lyp/+}$ and $DR^{+/+}$ control rats showed similar body weight, glucose levels, and islet morphology at any age. The body weight and blood glucose for each individual rat was recorded daily from 40 days of age until $DR^{lyp/lyp}$ rats became diabetic (blood glucose levels ≥250 mg/dl). Rat pancreata were processed for histological analysis or hormone assay. All animal studies were approved by the Institutional Animal Care and Use Committee of the University of Washington and BRI.

Histochemistry and immunohistochemistry Staining methodologies were performed as previously described [17]. Serial sections were prepared from all the paraffin blocks. Sections were stained for HA

using a biotinylated HA binding protein prepared from cartilage [24]. The primary antibodies used for immunohistochemistry are listed in ESM Table 2. Positive and negative controls were included in each staining experiment. Sections were examined using a Leica DM IRB microscope, and images were acquired using a Spot Xplorer camera and imaging software.

Morphometric analysis and quantification Whole-section bright-field imaging was performed as previously [17, 23]. Islets were identified by their staining for synaptophysin (SYN). Thirty percent of the human islets were sampled according to assumption-free systematic uniform random sampling, based on our pilot studies which indicate that this sampling results in a coefficient of error <2%. We classified the islet HA+ areas using an established categorization scheme with the following categories: <100, 100-500, 500-1000, 1000-2000, and >2000 μm^2 per islet [17, 25, 26]. Tissues from aAb+ donors with an average islet HA-stained area significantly larger than that of the aAb- controls were defined as aAb+HA^{high} or as having HA deposits, while tissues with islet HA-stained areas that were similar in size to those of the controls as aAb+HA^{low}.

Evaluation of islet immune cell infiltrates Sections were stained for LCA and SYN to detect islet-infiltrating immune cells. All the islets present in the sections were examined. Islets were counted along with the number of LCA+ cells in contact with the endocrine cells [17, 22]. Human islet immune cell infiltrates were evaluated by determining 1) the percentage of islets with LCA+ cells adjacent to endocrine cells, and 2) the number per islet of LCA+ cells in contact with endocrine cells. Tissues exhibiting ≥15 LCA+ cells per islet [9, 27] were defined as LCA^{high}. In $DR^{lyp/lyp}$ rats, insulitis is a continuum from scarce to numerous immune cells, which first appear at the islet periphery and subsequently invade the whole islet. In these rats, insulitis was evaluated according to the presence and the extent of islet LCA+ cell infiltration, and was graded as follows: grade 0, no infiltration; grade 1, LCA+ cells present around islets and within the islets in less than 25% of the islet area; grade 2, LCA+ cells occupying less than 75% of the islet area; and grade 3, LCA+ cells infiltrating more than 75% of the islet or islets devoid of beta cells.

Each islet in an individual rat was examined once and assigned an insulitis grade, and the grade of highest prevalence determined the insulitis grade for that rat (ESM Table 3). The control $DR^{lyp/+}$ and $DR^{+/+}$ rats do not develop insulitis.

Quantitation of islet mass, beta cell mass, proliferation, and apoptosis One section for each of the paraffin blocks sampled per human pancreas was stained for Ki67/insulin to determine the beta cell proliferation rate and to measure the relative insulin-positive area. Four sections per pancreas were stained for TUNEL/insulin to determine the apoptosis rate. The TUNEL stain (Millipore, MA, USA) was performed according to the manufacturer's instructions. For each rat, consecutive pancreas sections were stained for SYN (8 sections per rat, 400 µm apart) and insulin (8 sections per rat, 400 µm apart) to measure the relative pancreas islet and beta cell areas at 100% sampling using Visiopharm software. The relative positive areas were then multiplied by the pancreas weight to determine the islet or beta cell mass.

Statistical analysis Data are expressed as mean ± SEM of *n* independent measurements. Significance of the difference between two or more groups of data was evaluated using the Mann-Whitney *U* test, Kruskal-Wallis test, or ANOVA. Correlation analysis was performed using the nonparametric Spearman rank correlation test. A *p* value of less than 0.05 was considered statistically significant.

Results

Abundant islet HA deposits form in a subset of aAb+ donors While HA was detectable extracellularly in islets from all pancreas samples, islets from aAb+ donors exhibited HA deposits, defined by the greater areas of HA staining vs. controls (Fig. 1). Examination of 4598 islets from 14 aAb- and 5482 islets from 15 aAb+ donors indicated 2.8-fold larger islet HA-stained areas in the aAb+ group (Fig. 1c). This difference was due to a higher occurrence of larger areas of HA staining (>500 μm^2) and lower occurrence of smaller HA-stained areas (<500 μm^2) than in aAb- controls ($p<0.001$, one-way ANOVA). We used the range of HA-stained area in the control samples to define an upper cut-off value for "normal" HA staining,

set at three standard deviations above the mean of the controls, as it should include >99% of values typical of aAb- controls. Dividing the 15 aAb+ donors using this threshold yielded two distinct groups (Fig. 2e and ESM Fig. 1). One group of 8 aAb+ donors (aAb+HA^{low}) was not different from the aAb- controls, while the other 7 (aAb+HA^{high}) had HA deposits in their islets. These 7 donors were at different stages of islet autoimmunity, since 3 were single and 4 were double aAb+. In these donors, the islet HA-stained areas were 4-fold larger than in the other donors (Fig. 2). The aAb+HA^{high} tissues also showed a greater prevalence of islets highly rich in HA (17% of the islets contained largest HA-stained areas of >2000 μm^2 vs. less than 1% in the controls). Moreover, in these tissues, islet HA+ areas measuring 6000 to 28,000 μm^2 were frequently observed, while such areas were not present in the aAb- controls and aAb+HA^{low} tissues (ESM Fig. 1).

We found a positive association between the amount of islet HA staining and the number of aAbs but not the donor age (Fig. 2 and ESM Fig. 2b). The islet HA-stained areas in the single aAb+ donors were on average 1.6-fold greater than in the aAb- controls. This increase in size was attributable to the HA abundance in 3 single aAb+ donors which exhibited 2.7 and 3.4-fold larger islet HA-stained areas than those in aAb- or the other 6 single aAb+ donors (p<0.01). The double aAb+ group overall also exhibited larger amounts of islet HA staining compared to single aAb+ or aAb- groups. This was a result of the prominent HA deposition in 4 of the 5 donors in this group, which resulted in islet HA+ areas that were 4- and 5-fold larger than in single aAb+ donors or the aAb- controls, respectively (p<0.01). The increase in the islet HA area in the aAb+HA^{high} tissues was not determined by the islet size. Overall, the islet areas in the aAb+ donors were within the normal range of the aAb- control measurements (ESM Fig. 3).

Islet HA deposits form in the absence of insulitis and are the sites of immune cell infiltrates

Among the 7 aAb+HA^{high} tissues, 3 from single and one from double aAb+ donors did not show insulitis (Fig. 3). The scarce islet-associated LCA+ cells present in these 4 HA-rich tissues occurred single units. Insulitis was detected in the other 3 tissues from donors positive for two aAbs (Fig. 3c, d, g-i). In these 3

aAb+HA^{high}LCA^{high} tissues, HA had accumulated in the majority of the islets (Fig. 4 and ESM Fig. 4a). However, the LCA+ cells were located only in 13%, 14%, and 28% of the islets in each of these tissues. The markedly lower prevalence of islets with LCA+ cells vs. that of HA-rich islets indicates that HA accumulation progresses independently of immune cell infiltration even in those tissues that eventually develop insulitis. Further assessment of the islet HA amounts in relation to insulitis in the 3 aAb+HA^{high}LCA^{high} tissues revealed that the insulitis-free islets contained less HA staining than neighboring islets with insulitis, yet more than the islets in the other 4 aAb+HA^{high} tissues (3.4- and 2.4-fold, respectively, ESM Fig. 4b). Furthermore, the islet infiltrating immune cells were located almost exclusively in the islets with substantial amounts of islet HA deposits (Fig. 4 and ESM Fig. 4a). In the 3 aAb+HA^{high}LCA^{high} tissues, about one third of the islets, 60% of which hosted immune cells, exhibited HA-stained areas larger than 2000 μm^2. By contrast, such areas were found in only 8% of the islets in the 4 aAb+HA^{high} tissues without insulitis and their average size was significantly smaller (3200±800 μm^2 vs. 6600±4700 μm^2, p<0.001). In the 3 aAb+HA^{high}LCA^{high} tissues, CD68 and CD3+ cells were frequently found in islets with islet-associated LCA+ immune cells (ESM Fig. 4c). Scarce CD20+ or CD11c+ cells were detected in case 1 only, and were observed in the regions of insulitis together with other immune cells. These data may indicate that cells from both myeloid and lymphoid lineage might be attracted by islet HA. The lower frequency of CD20+ and CD11c+ cells vs. that of CD68+ or CD3+ cells may indicate that occurrence of the former may be determined by a specific composition of the HA-rich islet ECM and/or the presence of other immune cell types in islets.

The formation of large HA deposits in the 3 tissues with insulitis was not associated with greater numbers of LCA+ cells in the non-islet region. Also, the relative HA+ areas in the non-islet compartment in the aAb+HA^{high} group overall were not significantly different from those in the controls (ESM Fig. 2c and d).

Relationship of human islet HA to beta cell mass The formation of HA deposits in islets of aAb+ donors was not associated with changes in the size of the beta cell population (Fig. 5a-c). Apoptotic cells with

TUNEL-positive nuclei were not detected in the endocrine compartment in any of the tissues from either the aAb- or aAb+ groups. Also, the rate of beta cell proliferation did not differ between these two groups (0.1±0.1% in both). Beta cell mass varied among both aAb- and aAb+ donors and was not related to the extent of HA staining. Interestingly, there was little variation in the size of the relative pancreas insulin-positive areas, indicating that much of the variability in beta cell mass was due to differences in pancreas weight rather than islet density (Fig. 5d).

Islet HA deposits form in the presence of aAbs but are not HLA related Previous work indicated that the presence of islet aAbs is HLA-associated, while the progression from aAb positivity to clinical disease is not [28, 29]. Therefore, we next examined the extent of islet HA deposition in relation to HLA. Two of 9 donors with the HLA haplotype DR4-DQ8 (DRB1*04-DQA1*0301-DQB1*0302), which is strongly associated with T1D [30, 31], had substantial amounts of HA staining in their islets. Three of 12 donors with HLA haplotypes often considered protective for T1D (DRB1*0401-DQA1*0301-DQB1*0301, DRB1*1501-DQA1*0102-DQB1*0603, and DRB1*0401-DQA1*0301-DQB1*0301) and 2 of 7 with HLA haplotypes conferring neutral risk (DRB1*0101-DQA1*0101-DQB1*0501 and DRB1*0701-DQA1*0201-DQA2*0201) also exhibited larger HA+ areas in their tissues vs. controls (ESM Fig. 6 and ESM Table 1). Thus, overall, the presence of the HA-stained deposits was not associated with HLA haplotype.

In summary, as illustrated in Fig. 6, a subset of single and double aAb+ donors (cases 1 - 7) showed prominent islet HA deposits. The HA-rich tissues containing the largest quantities of HA in their islets (cases 1 - 3) exhibited insulitis. Tissues from the other aAb+ donors (cases 8 - 15), who were mostly single aAb, did not exhibit insulitis and did not differ from the aAb- controls with respect to the quantities and distribution of islet HA, or beta cell mass (ESM Fig. 6).

Islet HA deposition precedes insulitis in presymptomatic DR$^{lyp/lyp}$ rats The DR$^{lyp/lyp}$ rat islets were insulitic cell-free during the first 8 weeks of age (insulitis grade 0) (ESM Table 3). The insulitic infiltrates

appeared at 9-10 weeks of age (grade 1, inaugural insulitis). Subsequently, these infiltrates gradually expanded around and within islets (grade 2, invasive insulitis), and then spread throughout them (grade 3, destructive insulitis). In this last stage, the islets showed massive beta cell loss, which typically leads to hyperglycemia within 24-48 hours (ESM Fig. 7a, b) [22, 23]. We first examined whether HA accumulates in islets prior to the appearance of insulitic cells, and then assessed the initiation and progression of insulitis and the beta cell mass as a function of the amount of islet HA in $DR^{lyp/lyp}$ rats during the progression to hyperglycemia.

At 6 weeks of age, the quantities and distribution of islet HA staining in the $DR^{lyp/lyp}$ rats did not differ from those in the $DR^{lyp/+}$ or $DR^{+/+}$ controls (ESM Fig. 7c). Islet HA deposits had developed both around and within islets in 7-8-week-old $DR^{lyp/lyp}$ rats, which exhibited 3-fold and 2.4-fold larger islet HA+ areas compared to the 6-week-old $DR^{lyp/lyp}$ and control rats, respectively (Fig. 7 and ESM Fig. 8a, b). However, these rats did not show any islet-associated LCA+ cells (Fig. 7). Thus, in presymptomatic $DR^{lyp/lyp}$ rats, islet HA deposits form before the appearance of insulitic cells.

In the 9-10-week-old $DR^{lyp/lyp}$ rats, the islet HA-stained areas were on average twice as large as those of their $DR^{lyp/lyp}$ littermates at 7-8 weeks of age, while the SYN-positive areas were smaller (ESM Fig. 8f). This increase in size was due to a higher prevalence of islets rich in HA and the formation of large HA-deposits measuring 8000-16,000 μm^2, which were not present in younger rats (Fig. 7 and ESM Fig. 8). At this age the first insulitic cells appeared and were embedded within the largest HA accumulations. This suggests that the HA-rich areas are the sites of immune cell entry into islets. The islet HA+ areas were larger in $DR^{lyp/lyp}$ rats at 10-11 weeks of age (1.5-fold vs. 9-10-week-old $DR^{lyp/lyp}$ rats) and measured up to 30,000 μm^2, indicating a massive deposition of islet HA. This was associated with exacerbation of insulitis, since most islets exhibited a higher degree of immune cell infiltration.

The initial accumulation of HA in $DR^{lyp/lyp}$ rat islets was not associated with a significant loss of beta cells (Fig. 7 and ESM Fig. 8c). In rats exhibiting abundant islet HA-staining and grade 1 insulitis, the beta cell mass was reduced to 56% of that in the controls. With further expansion of the HA deposits and

progression to invasive insulitis, the size of beta cell population continued to decrease. HA remained abundant in rats with destructive insulitis, which had lost 60% of their islet mass (1±0.3 mg vs. 2.5±1 mg in DR$^{lyp/lyp}$ rats with grade 0 insulitis, p<0.01) and 85% of the beta cells (ESM Fig. 8c-e).

Discussion

HA is a major component of the ECM that amasses in chronic inflammatory lesions, where HA exerts proinflammatory effects as a key regulator of leukocyte recruitment to the site of injury [19, 20, 32-34]. Our previous observation of abundant HA in human islets and insulitis regions in type 1 diabetes implicated HA in the disease pathogenesis [17]. Here, we investigated whether the accumulation of HA in islets is an early and critical step in the pathogenetic process of the disease.

We report that HA deposits form in islets in a subset of aAb+ donors in the absence of insulitis. We also show that, on average, the double aAb+ donors exhibited larger islet HA deposits than those positive for a single aAb. These observations reveal that islet immune cell infiltrates are not required for the initial islet HA deposition, and that the islet HA deposits expand along with the increase in the number of islet aAbs indicating progression of autoimmunity. It is important to point out that the largest islet HA deposits and insulitis were observed in the double aAb+ donors who carried the highly susceptible genotype and were under 40 years of age. Essentially, all individuals with multiple islet aAbs subsequently progress to clinically overt diabetes [35]. Although progression to clinical onset of diabetes occurs at different rates, we suggest that the 7 aAb+ donors exhibiting prominent HA deposits were in a stage of rapid progression of the pathogenic process.

In presymptomatic DR$^{lyp/lyp}$ rats, the initial islet HA deposition predates the appearance of insulitic cells. This finding together with our observation of islet HA deposits in the absence of islet immune cell infiltrates in aAb+ donors indicates that the process of HA accumulation in islets can occur independently of and prior to insulitis. To what extent this accumulation would have eventually contributed to the development of insulitis in the subset of single aAb+ donors with islet HA deposits, had they lived longer,

is not possible to determine. Nonetheless, these results suggest that the formation of islet HA deposits may be a prerequisite for the initial adhesion of insulitic cells and subsequent infiltration of islets, and thus could potentially be considered causal. Support for an HA-insulitis causal relationship comes from in vitro studies which indicated that an HA-rich ECM generated by activated human fibroblasts, endothelial or smooth muscle cells, controls the migration of human mononuclear leukocytes [34, 36, 37]. Also, our observations in BB rats are in line with the finding of HA accumulation preceding the inflammatory infiltrate in the intestinal mucosa in mice with induced experimental colitis [38].

We point out a relationship between the extensiveness of islet HA accumulation and the degree of insulitis, as in BB rats the amount of islet HA staining positively correlates with the continuum of insulitis, from inaugural to invasive. The immune cells were first observed in DR$^{lyp/lyp}$ rats in which the islet HA-stained areas had increased on average 2.4-fold. Also, in both humans and BB rats, the immune cell infiltrates were situated within the largest HA accumulations in islets. These findings indicate that the precursory islet HA buildup may determine the sites of subsequent immune cell entry into islets, and that insulitis initiates in those islets which have accumulated a "critical" mass of HA. Additional islet HA deposition was concurrent with expansion of insulitic infiltrates inside islets, which suggests that the continuous amassment of HA may also influence the advancement of insulitis.

While the initial HA accumulation was not associated with a significant reduction in beta cell mass, the DR$^{lyp/lyp}$ rats with HA abundant deposits and grade1 insulitis exhibited a considerable loss of beta cells. The consequences of HA deposition on beta cell survival remain to be determined. In the presence of insulitis, it is difficult to dissect the impact of the accumulated HA from that of the immune cells [12, 39-41]. However, it can be speculated that changes in the islet ECM properties, conferred by continual HA deposition, might affect beta cell viability via HA-induced signaling pathways and cellular responses in islets. Also, abundant HA, in synergy with the insulitic cells and secreted cytokines, may create an inflammatory microenvironment that is detrimental to beta cells.

Human islets with abundant HA were not localized in specific parts of the human pancreas, and their uneven distribution is reminiscent of the "patchy" pattern of insulitis described in type 1 diabetes [1, 9, 11]. We previously found a similar distribution pattern of HA-rich islets and insulitis in human diabetic pancreata [17]. These observations were reproduced in prediabetic and diabetic BB rats in the present study, in which the location of the largest islet HA deposits served as a blueprint for islet immune cell infiltration. The complete overlap in the localization of islets highly enriched in HA and insulitis reinforces their close relationship, which, from initially being potentially causative, might have progressed into an interdependent partnership.

In conclusion, this study indicates that islet HA accumulation is an early event in the pathogenesis of autoimmune diabetes. Our novel observations, remarkably consistent in both humans with ongoing islet autoimmunity and diabetes-prone BB rats in the preclinical stage of the disease, support our proposal of a crucial role of islet HA in the inception and promotion of islet inflammation in type 1 diabetes [16]. Therefore, additional studies are warranted to explore the underlying mechanisms that regulate HA mass in islets and the interactions between HA and islet cells or immune cells. Clarifying these molecular mechanisms will be important in developing therapeutic interventions that target HA accumulation with the aim to stop the development of insulitis.

Acknowledgments This research was performed with the support of the Network for Pancreatic Organ Donors with Diabetes (nPOD), a collaborative type 1 diabetes research project sponsored by JDRF. Organ Procurement Organizations partnering with nPOD to provide research resources are listed at http://www.jdrfnpod.org/for-partners/npod-partners/. We thank Dr. Virginia Green (BRI) for editing the manuscript.

Data availability The data are available on request from the corresponding author.

Funding This study was supported by the Leona M. and Harry B. Helmsley Charitable Trust George S. Eisenbarth nPOD Award for Team Science to MB and TNW (2015PG T1D052) and by a Pilot Project to MB from the NIAID Cooperative Study Group for Autoimmune Disease Prevention Innovative Study (U01 AI101990). National Institutes of Health National Institute of Diabetes and Digestive and Kidney Diseases grant P30-DK-17047 to University of Washington Diabetes Research Center Imaging and Cell Function Analysis Core provided core support. Å.L. was supported by the Swedish Research Council and the Diabetesfonden.

Duality of Interest The authors declare that there is no duality of interest associated with this manuscript.

Contribution statement MB conceived the project, designed and performed the experiments, collected and analyzed the data, and wrote the manuscript. PYJ assisted with the immunohistochemistry experiments. MJD assisted with statistical analysis. MJL assisted with the morphometric measurements. AJD and TNW reviewed the manuscript. CS and CJG contributed to writing the manuscript. MB is the guarantor of this work. All authors approved the final version of the manuscript.

References

[1] Atkinson MA, Eisenbarth GS, Michels AW (2014) Type 1 diabetes. Lancet 383(9911): 69-82. 10.1016/S0140-6736(13)60591-7

[2] Eisenbarth GS (1986) Type I diabetes mellitus. A chronic autoimmune disease. N Engl J Med 314(21): 1360-1368. 10.1056/NEJM198605223142106

[3] Insel RA, Dunne JL, Atkinson MA, et al. (2015) Staging presymptomatic type 1 diabetes: a scientific statement of JDRF, the Endocrine Society, and the American Diabetes Association. Diabetes Care 38(10): 1964-1974. 10.2337/dc15-1419

[4] Couper JJ, Haller MJ, Greenbaum CJ, et al. (2018) ISPAD Clinical Practice Consensus Guidelines 2018: Stages of type 1 diabetes in children and adolescents. Pediatr Diabetes 19 Suppl 27: 20-27. 10.1111/pedi.12734

[5] Bingley PJ, Bonifacio E, Williams AJ, Genovese S, Bottazzo GF, Gale EA (1997) Prediction of IDDM in the general population: strategies based on combinations of autoantibody markers. Diabetes 46(11): 1701-1710

[6] Gorus FK, Keymeulen B, Veld PA, Pipeleers DG (2013) Predictors of progression to Type 1 diabetes: preparing for immune interventions in the preclinical disease phase. Expert Rev Clin Immunol 9(12): 1173-1183. 10.1586/1744666X.2013.856757

[7] Ziegler AG, Rewers M, Simell O, et al. (2013) Seroconversion to multiple islet autoantibodies and risk of progression to diabetes in children. JAMA 309(23): 2473-2479. 10.1001/jama.2013.6285

[8] Wherrett DK, Chiang JL, Delamater AM, et al. (2015) Defining pathways for development of disease-modifying therapies in children with type 1 diabetes: a consensus report. Diabetes Care 38(10): 1975-1985. 10.2337/dc15-1429

[9] Gepts W (1965) Pathologic anatomy of the pancreas in juvenile diabetes mellitus. Diabetes 14(10): 619-633

[10] Pipeleers D, Ling Z (1992) Pancreatic beta cells in insulin-dependent diabetes. Diabetes Metab Rev 8(3): 209-227

[11] In't Veld P (2011) Insulitis in human type 1 diabetes: The quest for an elusive lesion. Islets 3(4): 131-138

[12] Roep BO (2003) The role of T-cells in the pathogenesis of Type 1 diabetes: from cause to cure. Diabetologia 46(3): 305-321. 10.1007/s00125-003-1089-5

[13] Coppieters KT, Dotta F, Amirian N, et al. (2012) Demonstration of islet-autoreactive CD8 T cells in insulitic lesions from recent onset and long-term type 1 diabetes patients. J Exp Med 209(1): 51-60. 10.1084/jem.20111187

[14] Campbell-Thompson M, Fu A, Kaddis JS, et al. (2016) Insulitis and beta-Cell Mass in the Natural History of Type 1 Diabetes. Diabetes 65(3): 719-731. 10.2337/db15-0779

[15] Morgan NG, Richardson SJ (2018) Fifty years of pancreatic islet pathology in human type 1 diabetes: insights gained and progress made. Diabetologia. 10.1007/s00125-018-4731-y

[16] Bogdani M (2016) Thinking outside the cell: a key role for hyaluronan in the pathogenesis of human type 1 diabetes. Diabetes 65(8): 2105-2114. 10.2337/db15-1750

[17] Bogdani M, Johnson PY, Potter-Perigo S, et al. (2014) Hyaluronan and hyaluronan-binding proteins accumulate in both human type 1 diabetic islets and lymphoid tissues and associate with inflammatory cells in insulitis. Diabetes 63(8): 2727-2743. 10.2337/db13-1658

[18] Laurent TC, Laurent UB, Fraser JR (1996) The structure and function of hyaluronan: An overview. Immunol Cell Biol 74(2): A1-7. 10.1038/icb.1996.32

[19] Petrey AC, de la Motte CA (2014) Hyaluronan, a crucial regulator of inflammation. Front Immunol 5: 101. 10.3389/fimmu.2014.00101

[20] Wang A, de la Motte C, Lauer M, Hascall V (2011) Hyaluronan matrices in pathobiological processes. FEBS J 278(9): 1412-1418. 10.1111/j.1742-4658.2011.08069.x

[21] Mordes JP, Bortell R, Blankenhorn EP, Rossini AA, Greiner DL (2004) Rat models of type 1 diabetes: genetics, environment, and autoimmunity. ILAR J 45(3): 278-291

[22] Fuller JM, Bogdani M, Tupling TD, et al. (2009) Genetic dissection reveals diabetes loci proximal to the gimap5 lymphopenia gene. Physiological genomics 38(1): 89-97. 10.1152/physiolgenomics.00015.2009

[23] Bogdani M, Henschel AM, Kansra S, et al. (2013) Biobreeding rat islets exhibit reduced antioxidative defense and N-acetyl cysteine treatment delays type 1 diabetes. J Endocrinol 216(2): 111-123. 10.1530/joe-12-0385

[24] Toole BP, Yu Q, Underhill CB (2001) Hyaluronan and hyaluronan-binding proteins. Probes for specific detection. Methods Mol Biol 171: 479-485. 10.1385/1-59259-209-0:479

[25] Hellman B, Angervall L (1961) The frequency distribution of the number and volume of the islets of Langerhans in man. 3. Studies in diabetes of early onset, insuloma and acromegaly. Acta Pathol Microbiol Scand 53: 230-236. 10.1111/j.1699-0463.1961.tb00405.x

[26] Kim A, Miller K, Jo J, Kilimnik G, Wojcik P, Hara M (2009) Islet architecture: A comparative study. Islets 1(2): 129-136. 10.4161/isl.1.2.9480

[27] Campbell-Thompson ML, Atkinson MA, Butler AE, et al. (2013) The diagnosis of insulitis in human type 1 diabetes. Diabetologia 56(11): 2541-2543. 10.1007/s00125-013-3043-5

[28] Ziegler AG, Nepom GT (2010) Prediction and pathogenesis in type 1 diabetes. Immunity 32(4): 468-478. 10.1016/j.immuni.2010.03.018

[29] Redondo MJ, Geyer S, Steck AK, et al. (2018) A Type 1 Diabetes Genetic Risk Score Predicts Progression of Islet Autoimmunity and Development of Type 1 Diabetes in Individuals at Risk. Diabetes Care 41(9): 1887-1894. 10.2337/dc18-0087

[30] Concannon P, Rich SS, Nepom GT (2009) Genetics of type 1A diabetes. N Engl J Med 360(16): 1646-1654. 10.1056/NEJMra0808284

[31] Noble JA, Erlich HA (2012) Genetics of type 1 diabetes. Cold Spring Harb Perspect Med 2(1): a007732. 10.1101/cshperspect.a007732

[32] Jiang D, Liang J, Noble PW (2011) Hyaluronan as an immune regulator in human diseases. Physiol Rev 91(1): 221-264. 10.1152/physrev.00052.2009

[33] Mummert ME (2005) Immunologic roles of hyaluronan. Immunol Res 31(3): 189-206. 10.1385/IR:31:3:189

[34] Evanko SP, Potter-Perigo S, Bollyky PL, Nepom GT, Wight TN (2012) Hyaluronan and versican in the control of human T-lymphocyte adhesion and migration. Matrix Biol 31(2): 90-100. 10.1016/j.matbio.2011.10.004

[35] Bingley PJ, Boulware DC, Krischer JP, Type 1 Diabetes TrialNet Study Group (2016) The implications of autoantibodies to a single islet antigen in relatives with normal glucose tolerance: development of other autoantibodies and progression to type 1 diabetes. Diabetologia 59(3): 542-549. 10.1007/s00125-015-3830-2

[36] de La Motte CA, Hascall VC, Calabro A, Yen-Lieberman B, Strong SA (1999) Mononuclear leukocytes preferentially bind via CD44 to hyaluronan on human intestinal mucosal smooth muscle cells after virus infection or treatment with poly(I.C). J Biol Chem 274(43): 30747-30755

[37] Lauer ME, Mukhopadhyay D, Fulop C, de la Motte CA, Majors AK, Hascall VC (2009) Primary murine airway smooth muscle cells exposed to poly(I,C) or tunicamycin synthesize a leukocyte-adhesive hyaluronan matrix. J Biol Chem 284(8): 5299-5312. 10.1074/jbc.M807965200

[38] Kessler S, Rho H, West G, Fiocchi C, Drazba J, de la Motte C (2008) Hyaluronan (HA) deposition precedes and promotes leukocyte recruitment in intestinal inflammation. Clin Transl Sci 1(1): 57-61. 10.1111/j.1752-8062.2008.00025.x

[39] Delaney CA, Pavlovic D, Hoorens A, Pipeleers DG, Eizirik DL (1997) Cytokines induce deoxyribonucleic acid strand breaks and apoptosis in human pancreatic islet cells. Endocrinology 138(6): 2610-2614. 10.1210/endo.138.6.5204

[40] Eizirik DL, Mandrup-Poulsen T (2001) A choice of death--the signal-transduction of immune-mediated beta-cell apoptosis. Diabetologia 44(12): 2115-2133. 10.1007/s001250100021

[41] Pinkse GG, Tysma OH, Bergen CA, et al. (2005) Autoreactive CD8 T cells associated with beta cell destruction in type 1 diabetes. Proc Natl Acad Sci U S A 102(51): 18425-18430. 10.1073/pnas.0508621102

Figure Legends

Fig. 1 Islet HA deposits in aAb+ donors. HA staining (brown) in islets from (**a**) aAb- and (**b**) aAb+ donors. Arrows indicate HA occurring at islet periphery (yellow arrows) or within the islet (light blue arrows). Arrowheads point to the islet border. Scale bars, 50 µm. (**c**) Violin plots of the individual HA+ areas in 4598 and 5482 islets analyzed in tissues from 14 aAb- and 15 aAb+ donors, respectively. (**d**) Violin plots of the individual HA+ areas measured in islets from each donor. Blue circles, aAb- donors; light red circles, single aAb+; dark red circles, double aAb+.

Fig. 2 HA accumulates in islets from a subset of aAb+ donors. HA staining (brown) in islets from (**a**) aAb-, (**b, c**) single aAb+, and (**d**) double aAb+ donors. Arrowheads point to the islet border. Scale bars, 50 µm. (**e**) Morphometric quantification of islet HA+ areas. Each circle denotes an individual donor. Blue circles, aAb- donors; light red circles, single aAb+; dark red circles, double aAb+. Data are mean values of islet HA+ areas for each individual donor. The numbers 1-7 indicate the aAb+HA^{high} tissues ranked according to the size of their islet HA+ areas. The dotted line indicates the upper cut-off value (mean + 3SD) of the measurements obtained from the aAb- controls. 4598, 3210, and 2272 islets from aAb-, single aAb+, and double aAb+ donor tissues were analyzed, respectively. *p<0.001, single aAb+ or double aAb+ vs. aAb-, Mann-Whitney U test. (**f**) Islet HA+ area size distribution. The pie charts represent the percentage of islets with HA+ areas falling within each of the HA+ area size categories. 4598, 982, and 1828 islets were analyzed in aAb- and aAb+HA^{high} tissues from 3 single and 4 double aAb+ donors, respectively.

Fig. 3 Islet HA accumulation takes place in the absence of insulitis. HA staining (brown) in islets from (**a**) aAb- and (**b-d**) aAb+ donors. Arrowheads point to the islet border. (**e-h**) Adjacent sections of the islets shown in (**a-d**) stained for LCA (brown) and SYN (red). The area of insulitis in (**d**) is shown magnified in the inset. Scale bars, 50 µm. (**i**) Prevalence of islets with LCA+ cell infiltrates plotted as a function of islet HA+ areas. Each circle denotes an individual donor. Data are mean values of measurements for each

individual donor. The dotted lines indicate the upper cut-off values (mean + 3SD) of the measurements obtained from the aAb- controls. The numbers 1-7 indicate the aAb+HA^{high} tissues ranked according to the size of their islet HA+ areas. Blue circles, aAb- donors; light red circles, single aAb+; dark red circles, double aAb+.

Fig.4 Insulitis occurs exclusively in the islet regions containing the largest HA deposits. Violin plots of HA+ areas in islets without (LCA-) or with (LCA+) immune cells. The total number of LCA- or LCA+ islets in each group is indicated.

Fig. 5 Relationship of islet HA to beta cell mass. Immunohistochemical staining for insulin in islets from (**a**) control aAb- and (**b**) aAb+HA^{high} tissues. Scale bars, 100 µm. (**c**) Individual measurements of beta cell mass plotted as a function of islet HA+ area. (**d**) Insulin-positive areas relative to the pancreas section areas. Data are mean values of measurements for each individual donor. The horizontal lines represent the average value in each group. The numbers 1-7 indicate the aAb+HA^{high} cases ranked according to the size of their islet HA+ areas. Blue circles, aAb- donors; light red circles, single aAb+; dark red circles, double aAb+.

Fig. 6 **(a)** Islet HA+ areas, insulitis, and beta cell mass in individual aAb+ donors. Islet HA+ areas are mean values of measurements obtained from the islets examined in each pancreas. The pie charts represent the percentage of islets with HA+ areas falling within each of the HA+ area size categories or the percentage of islets with LCA+ cells. The size of each red circle is proportional to the average size of the HA+ areas or to beta cell mass, which is indicated by the value number within the circle. Between 250 and 560 islets were analyzed per pancreas. See also ESM Fig. 6. N/D, not determined. (**b**) Whole slide images of pancreas tissue sections from case 1 (aAb+HA^{high}, left) and case 13 (aAb+HA^{low}, right). The blue, green, and red circles were drawn around the islet border and label islets with HA-stained areas <500 µm^2, 500-2000 µm^2, and >2000 µm^2, respectively. Scale bars, 2000 µm.

Fig. 7 Islet HA accumulation precedes insulitis in presymptomatic DR$^{lyp/lyp}$ rats. HA staining (brown) in islets from (**a**) diabetes-resistant DR$^{lyp/+}$ and (**b-e**) diabetes-prone DR$^{lyp/lyp}$ rats. Arrowheads point to the islet border. SYN (brown) staining of islets from (**f**) DR$^{lyp/+}$ and (**g-j**) DR$^{lyp/lyp}$ rats. Scale bars, 50 µm. (**k**) Islet HA+ areas, (**l**) islet HA+ area size distribution, (**m**) insulitis, and (**n**) beta cell mass in DR$^{lyp/+}$ (blue) and DR$^{lyp/lyp}$ (light blue and green) rats. Data in (**k**) are mean values of HA+ areas measured in 300-400 islets per group. The pie charts in (**l**) represent the percentage of islets with HA+ areas falling within each of the HA area size categories. The size of each circle in (**k**) and (**n**) is proportional to the average size of the HA+ areas or beta cell mass, which is indicated by the value number within the circle. Data in (**m**) represent the proportion of islets with insulitis grade 0, 1, 2 or 3 in the rats within each age group. See also ESM Table 3.

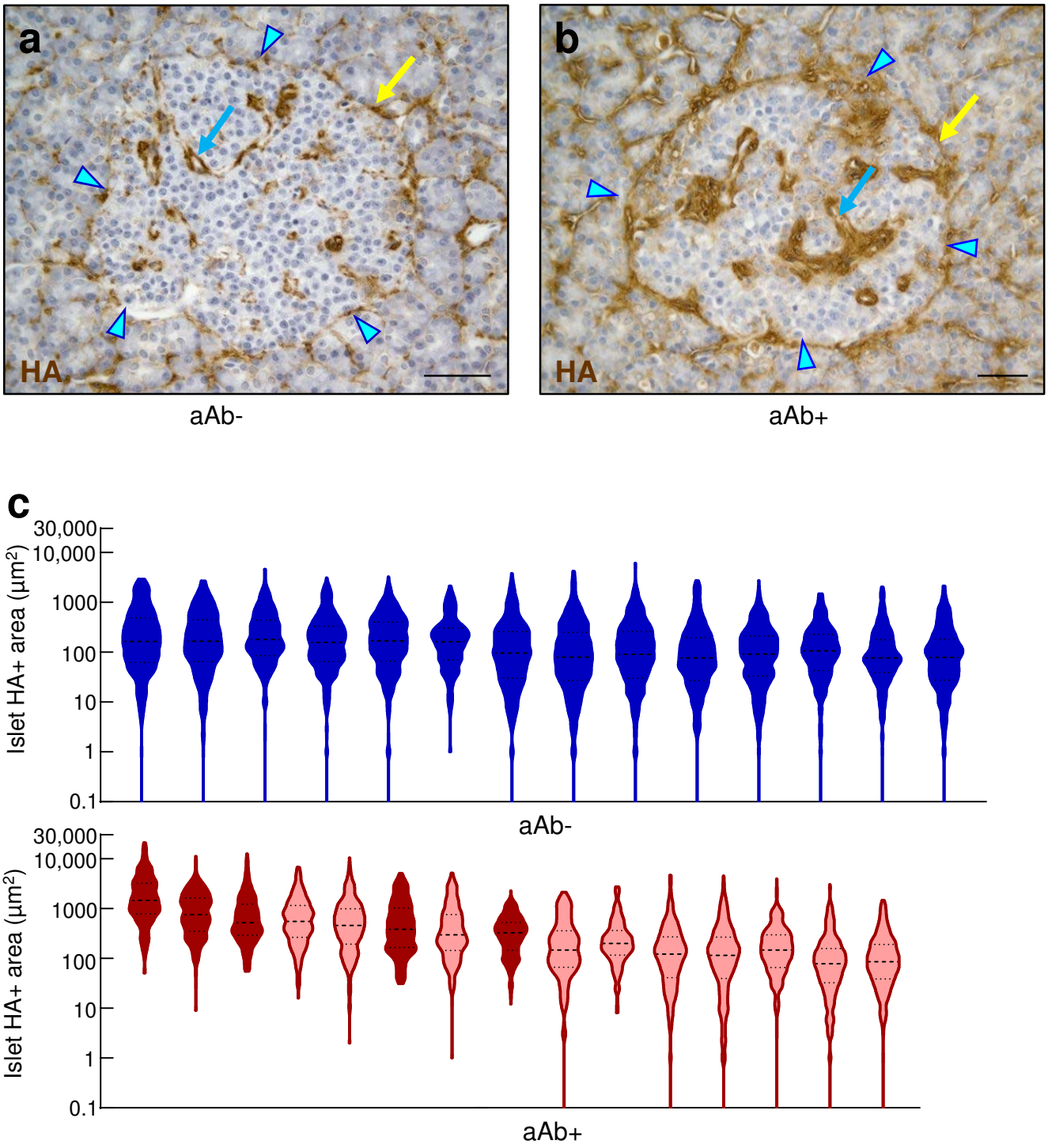

Figure 1 **Bogdani**

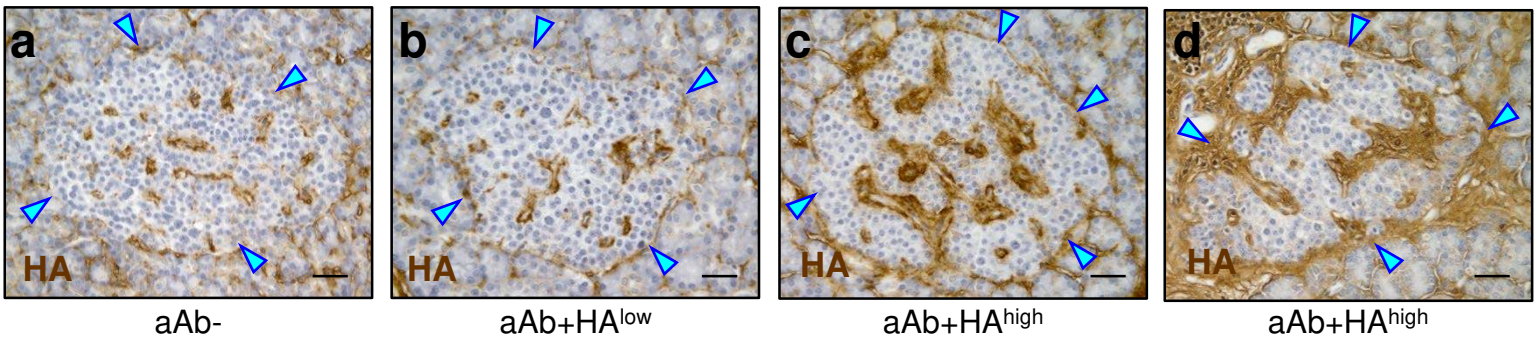

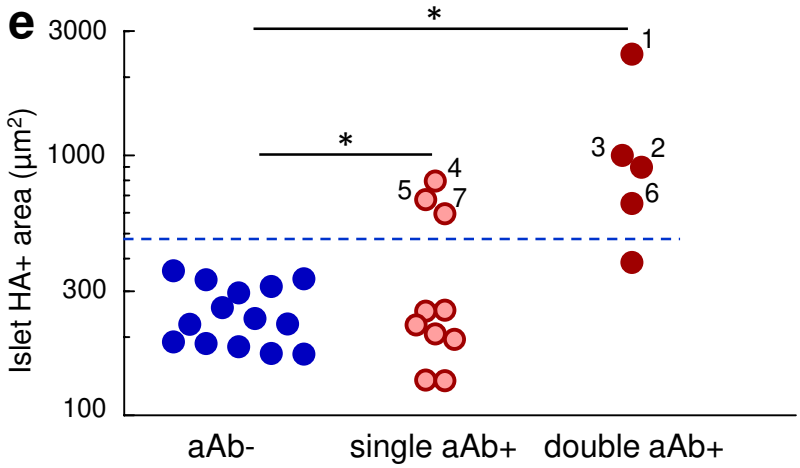

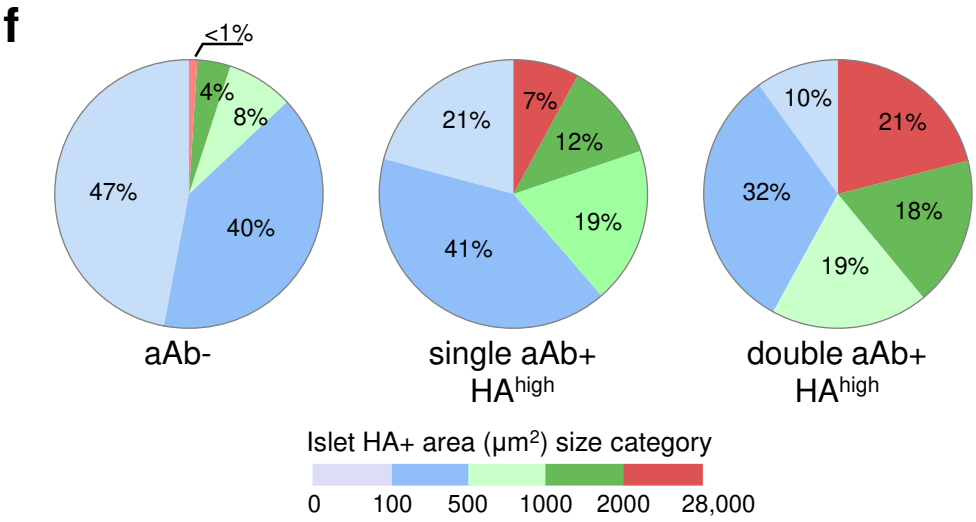

Figure 2 Bogdani

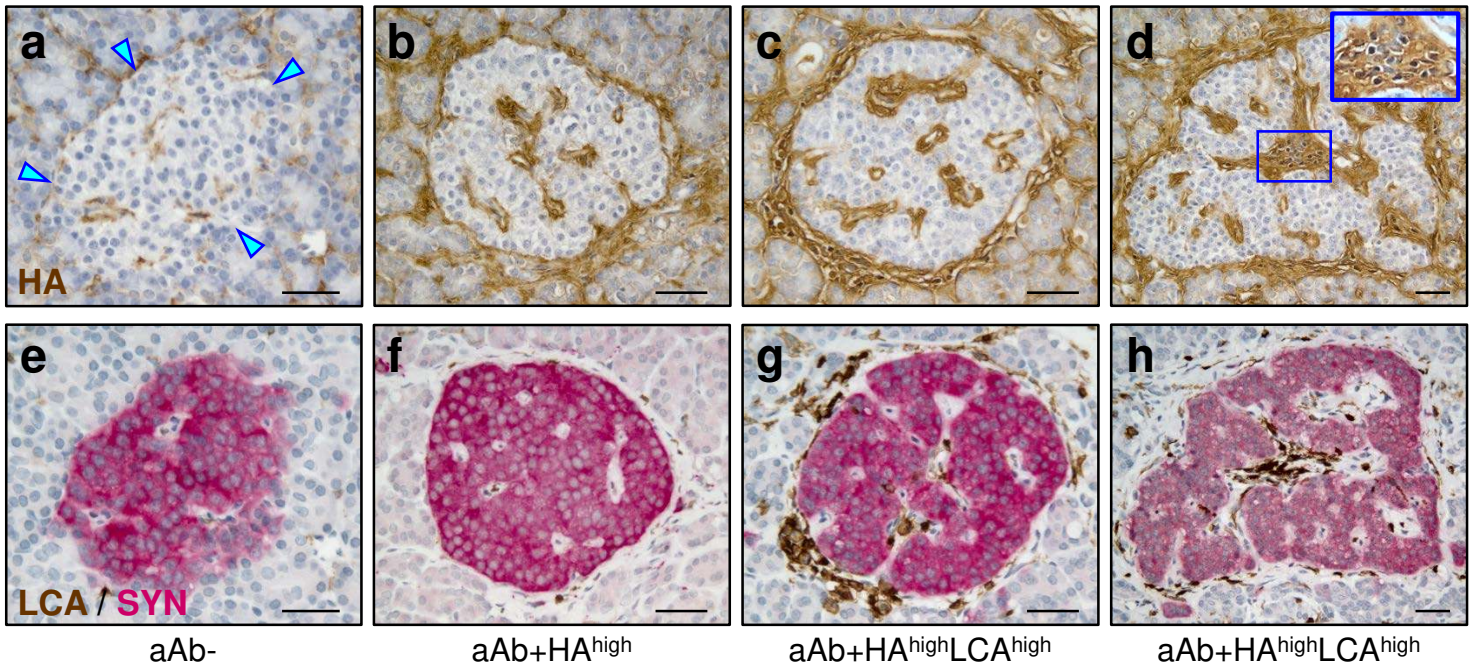

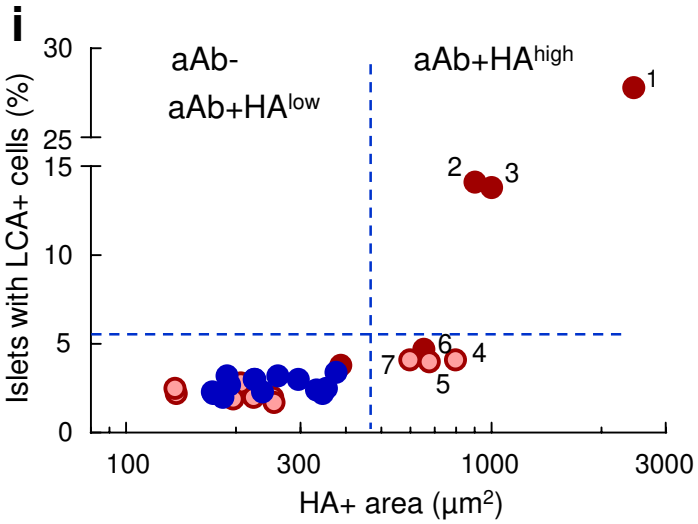

Figure 3 Bogdani

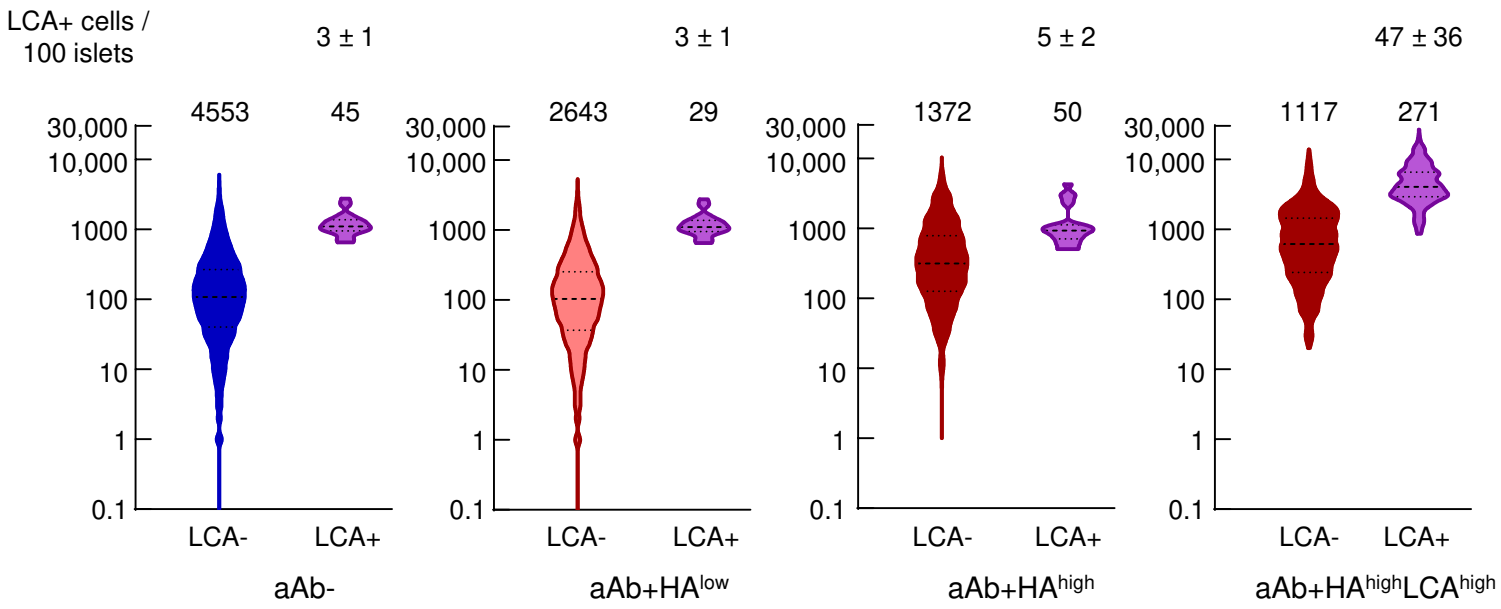

Figure 4 Bogdani

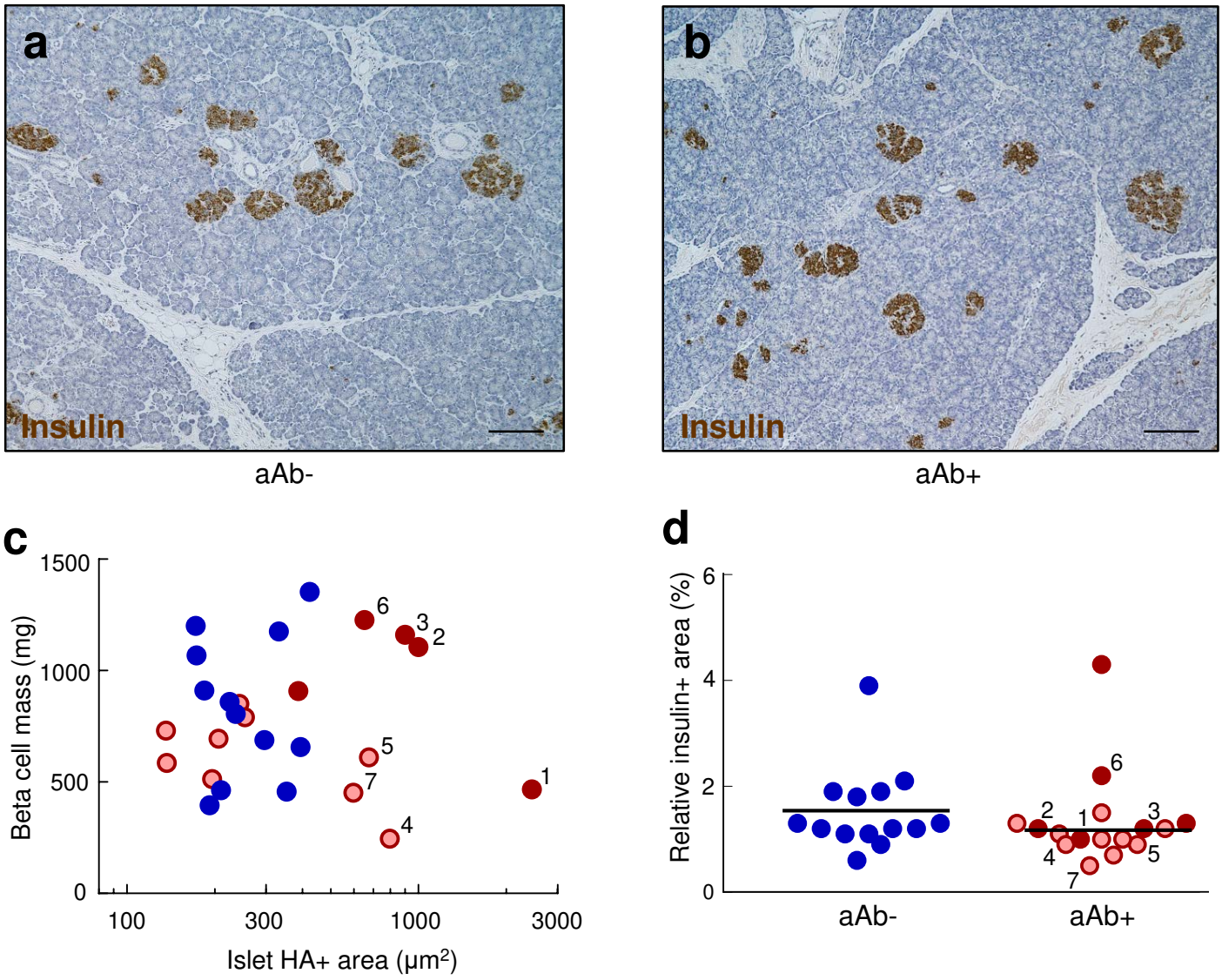

Figure 5 Bogdani

Figure 6 **Bogdani**

b

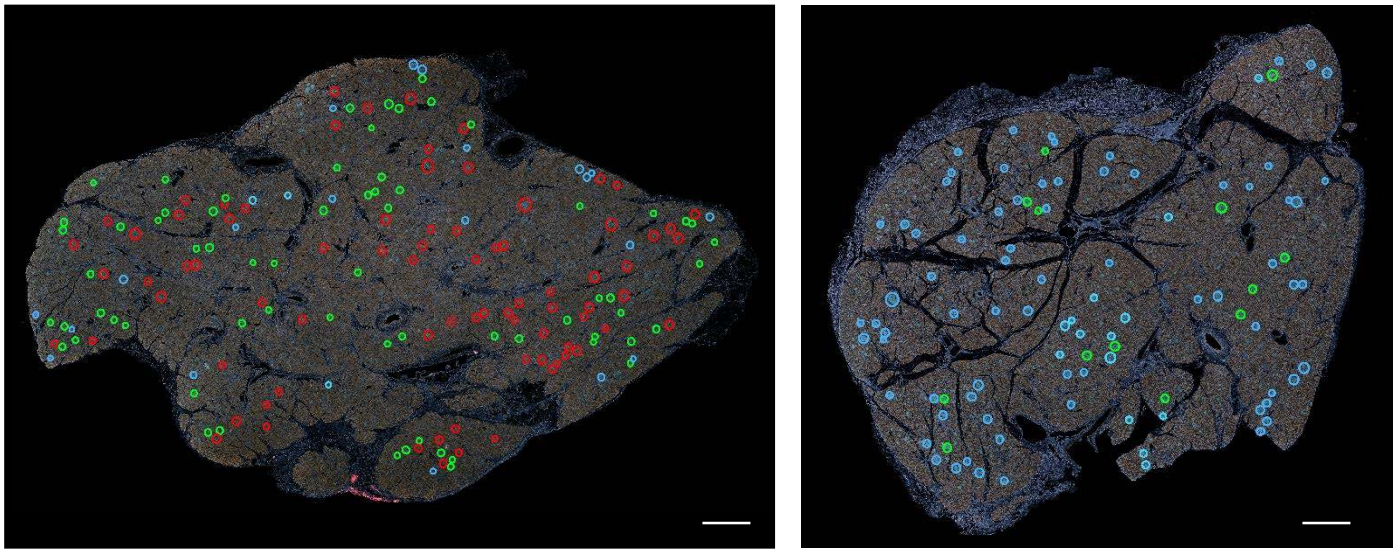

Figure 6 (cont'd) Bogdani

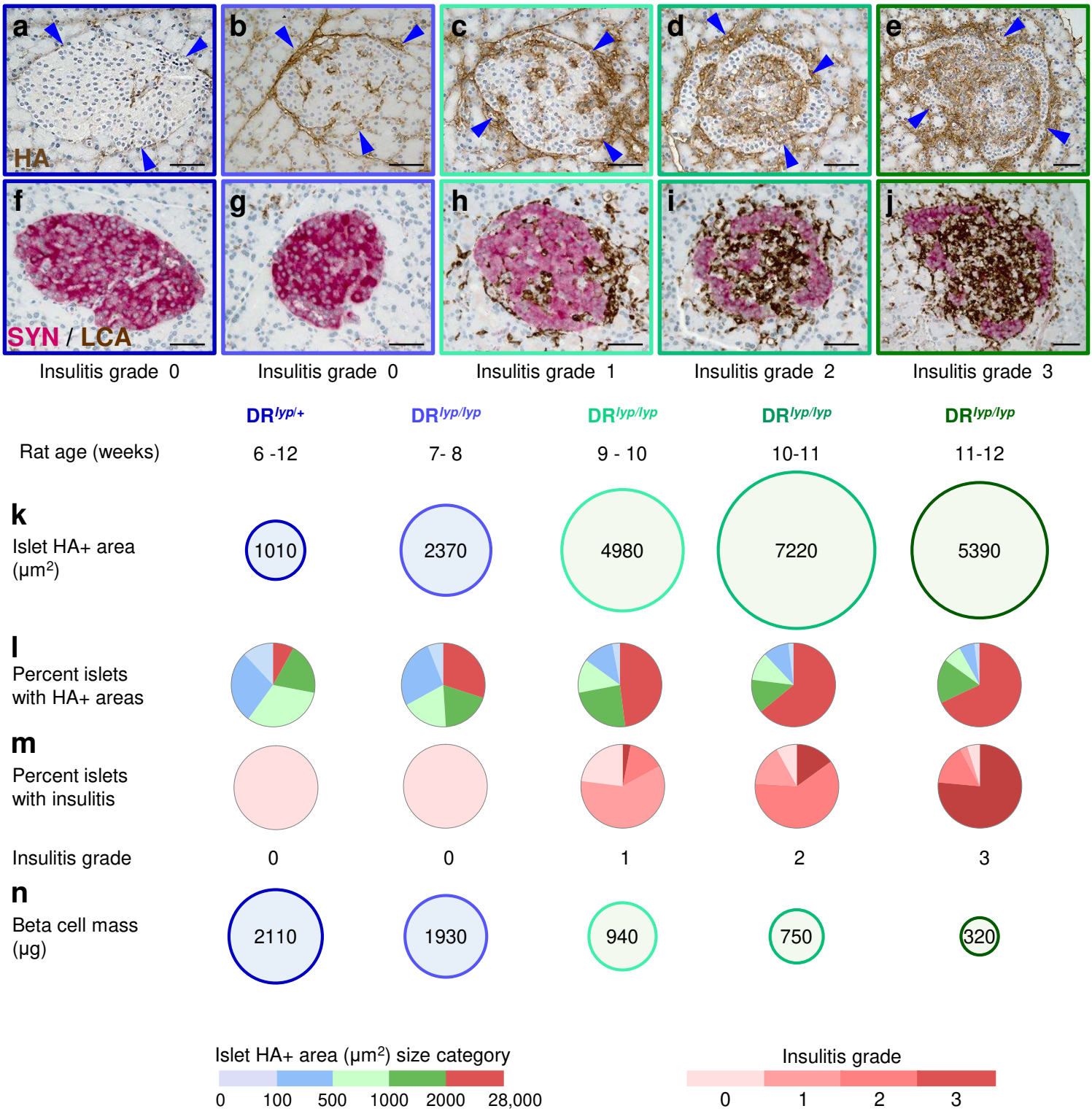

Figure 7 Bogdani

Electronic supplementary material (ESM)

Hyaluronan deposition in islets may precede and direct the location of islet immune cell infiltrates

Marika Bogdani, Cate Speake, Mathew J. Dufort, Pamela Y. Johnson, Megan J. Larmore, Anthony J. Day, Thomas N. Wight, Åke Lernmark, and Carla J. Greenbaum

ESM Table 1. Clinical and morphologic characteristics of study cases

Case	Case ID	Autoantibody	Age (years)	Gender	Ethnicity	C-peptide (ng/ml)	BMI	DRB1_1	DRB1_2	DQA1_1	DQA1_2	DQB1_1	DQB1_2	RISK (genotype)	RISK (haplotypes)	Family history for diabetes	Cause of death	Case group	Islet HA+ area (um2)	Beta cell mass (mg)
Autoantibody-positive																				
1	6267	GADA+ IA-2A+	23	Female	Caucasian	16.6	24	0401	0404	0301	0301	0302	0302	S	S / S	nr	Anoxia	$HA^{high}LCA^{high}$	2450	470
2	6167	IA2A+ ZnT8A+	37	Male	Caucasian	5.4	26	0404	1502	0103	0301	0302	0601	S	S / N	nr	Head trauma	$HA^{high}LCA^{high}$	1000	1100
3	6158	GADA+ mIAA+	40	Male	Caucasian	0.5	30	0401	1302	0102	0301	0301	0604	P	P / N	Father with T2D	Head trauma	$HA^{high}LCA^{high}$	900	1160
4	6154	GADA+	49	Female	Caucasian	0.1	25	0901	1501	0102	0301	0303	0603	P	N / P	nr	Head trauma	HA^{high}	800	610
5	6310	GADA+	28	Female	Hispanic	10.5	24	0701	1102	0201	0501	0202	0319	N	N / N	nr	Anoxia	HA^{high}	680	450
6	6197	GADA+ IA-2A+	22	Male	African-American	17.5	28	0302	0701	02:01	0401	0202	0402	P	P / P	Yes, unspecified	Head trauma	HA^{high}	660	1230
7	6151	GADA+	30	Male	Caucasian	5.5	24	0101	0701	0101	0201	0202	0501	N	N / N	nr	Anoxia	HA^{high}	600	240
8	6080	GADA+ mIAA+	69	Female	Caucasian	1.84	21	0101	0401	0101	0301	0301	0501	P	N / P	nr	Cerebrovascular/ stroke	HA^{low}	380	910
9	6027	ZnT8+	19	Male	Caucasian	nd	20	0301	1501	0102	0501	0201	0602	P	S / P	nr	nr	HA^{low}	250	790
10	6171	GADA+	4	Female	Caucasian	9.0	15	0301	0301	0501	0501	0201	0201	S	S / S	nr	Anoxia	HA^{low}	250	N/D
11	6303	GADA+	22	Male	Caucasian	3.0	32	0301	0701	0201	0501	0201	0202	S	S / N	Sister with juvenile T1D, father with T2D	Head trauma	HA^{low}	220	850
12	6181	GADA+	32	Male	Caucasian	0.6	22	0101	0401	0101	0301	0302	0501	S	N / S	nr	Head trauma	HA^{low}	200	690
13	6123	GADA+	23	Female	Caucasian	2.0	18	0801	1101	0401	0501	0301	0402	N	N / P	nr	Head trauma	HA^{low}	200	510
14	6301	GADA+	26	Male	African-American	3.9	32	1101	1304	0102	0501	0319	0602	P	P / P	nr	Head trauma	HA^{low}	140	580
15	6314	GADA+	21	Male	Caucasian	1.5	24	0103	0401	0101	0501	0301	0501	P	N / P	Yes, unspecified	Head trauma	HA^{low}	140	730
Average			30 ± 15	Females, 40%		6 ± 6	24 ± 5													
Autoantibody-negative																				
16	6055	Negative	27	Male	Caucasian	0.6	23	0103	0103	0501	0501	0301	0301	P	P / P	nr	Anoxia		180	1350
17	6104	Negative	41	Male	Caucasian	20.6	21	0701	1301	0101	0201	0201	0501	N	N / N	nr	Anoxia		350	450
18	6179	Negative	20	Female	Caucasian	2.7	21	0301	0404	0301	0501	0201	0302	S	S / S	nr	Head trauma		220	660
19	6233	Negative	14	Male	Caucasian	7.3	22	0101	1301	0101	0103	0501	0603	P	N / P	Mother and sister with T1D	Anoxia		330	1180
20	6129	Negative	43	Female	Caucasian	0.5	23	0301	1501	0102	0501	0201	0602	P	P / P	nr	Anoxia		230	690
21	6013	Negative	65	Male	Caucasian	2.8	24	0102	1301	0101	0103	0501	0603	N	N / P	nr	Cerebrovascular/ stroke		370	N/D
22	6230	Negative	16	Male	Caucasian	5.2	19	0401	1101	0301	0501	0301	0302	S	S / P	nr	Head trauma		190	800
23	6174	Negative	21	Male	Caucasian	3.0	20	0301	0701	0201	0501	0201	0201	S	S / N	nr	Cerebrovascular/ stroke		340	860
24	6232	Negative	14	Female	Caucasian	19.5	21	1501	1501	0102	0102	0602	0602	P	P / P	nr	Head trauma		180	460
25	6295	Negative	47	Female	African-American	10.9	30	0301	1501	0102	0501	0201	0602	P	S / P	nr	Head trauma		220	390
26	6005	Negative	5	Female	Caucasian	nd	nd	0101	1201	0101	0501	0301	0501	N	N / N	nr	Cerebrovascular/ stroke		170	N/D
27	6134	Negative	27	Male	Caucasian	3.6	20	0701	1001	0101	0201	0201	0501	N	N / N	nr	Anoxia		290	910
28	6160	Negative	22	Male	Caucasian	0.4	24	nd								nr	Head trauma		260	1070
29	6098	Negative	18	Male	Caucasian	1.4	23	0301	0801	0401	0501	0201	0402	S	S / N	nr	Head trauma		170	1200
Average			27 ± 16	Females, 30%		6 ± 7	22 ± 3													

nr, not reported
nd, not determined
P, protective; N, neutral; S, susceptible

Note 1. The case numbers indicate the tissues from autoantibody-positive and autoantibody-negative donors, which are ranked according to the size of their islet HA-positive areas, with 1 and 17 having the most HA in their respective groups.
Note 2. Numbers 1 - 7 are the aAb+HAhigh cases; numbers 8-16 are the aAb+HAlow cases.
Note 3. C-peptide levels are in ng/ml.

ESM Table 2. Primary antibodies used for immunohistochemistry.

Antigen	Antibody supplier	Catalog number	Dilution
Insulin	Abcam	ab7842	1:1000
Synaptophysin	Invitrogen	MA5-11575	1:100
Ki67	Abcam	ab15580	1:100
CD3	DAKO	A0452	1:100
CD11c	Abcam	ab52632	1:50
CD20	DAKO	M0755	1:50
CD68	DAKO	M0814	1:100
LCA	Abcam	ab187271	1:200
LCA (clone OX-1)	Bio-Rad	MCA43	1:100
CD68 (clone ED1)	Bio-Rad	MCA341	1:100

ESM Table 3. Insulitis grade, islet HA areas, and beta cell mass in BB rats.

Genotype	Age (weeks)	n	Percent islets with insulitis grade				Overall Insulitis grade	Islet HA area (μm^2)	Beta cell mass (µg)
			0	1	2	3			
$DR^{lyp}/+$	7		100	0	0	0	0	960	1520
	7		100	0	0	0	0	1140	2380
	7		100	0	0	0	0	1070	2520
	7		100	0	0	0	0	910	1420
	8		100	0	0	0	0	1030	2100
	8		100	0	0	0	0	930	2700
	7-8	6	100	0	0	0	0	1010	2110
$DR^{lyp}/^{lyp}$	7		100	0	0	0	0	1400	2080
	7		100	0	0	0	0	2250	2650
	7		100	0	0	0	0	3860	1100
	7		100	0	0	0	0	1790	2010
	8		100	0	0	0	0	2540	1800
	8		100	0	0	0	0	2380	1910
	7-8	6	100	0	0	0	0	2370	1930
$DR^{lyp}/^{lyp}$	9		21	69	8	2	1	4190	950
	9		25	67	8	0	1	3730	1180
	9		26	72	2	0	1	4610	780
	9		26	63	10	1	1	4490	750
	10		16	73	11	0	1	7950	840
	10		25	68	6	1	1	4900	1120
	9-10	6	23	69	8	1	1	4980	940
$DR^{lyp}/^{lyp}$	10		4	9	79	8	2	9040	470
	11		8	28	50	14	2	5280	550
	11		13	5	66	16	2	9640	610
	11		3	25	62	10	2	6270	1050
	11		12	15	61	12	2	5890	1090
	10-11	5	8	16	64	12	2	7220	750
$DR^{lyp}/^{lyp}$	11		1	1	29	69	3	5620	130
	11		5	3	2	90	3	3320	230
	12		6	2	7	93	3	4620	170
	12		0	1	19	80	3	4100	490
	12		2	0	28	70	3	8120	260
	12		8	2	10	80	3	6550	630
	11-12	6	4	2	16	80	3	5390	320

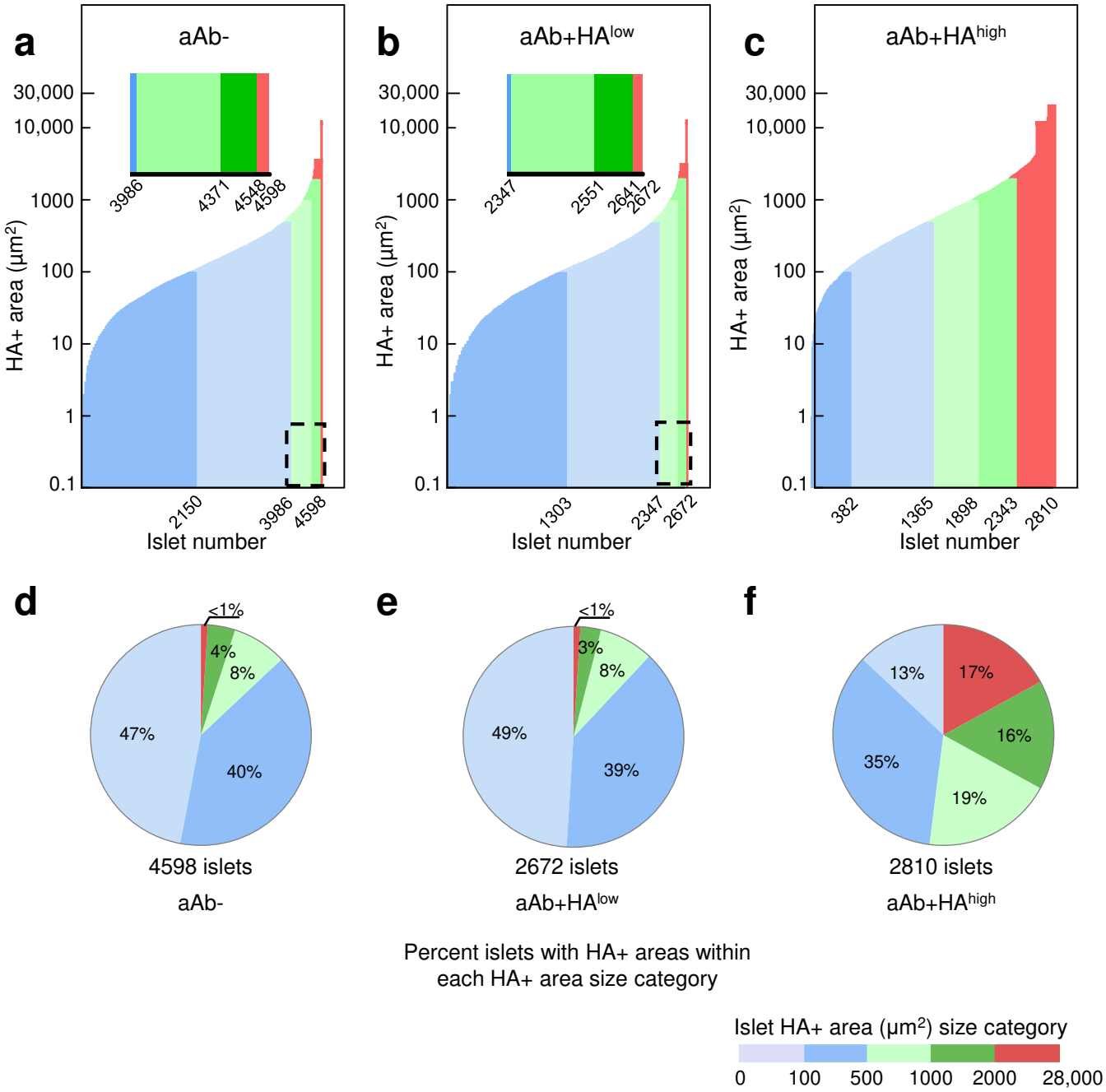

ESM Fig. 1 HA accumulates in islets in a subset of aAb+ donors. (**a-c**) Histograms of individual HA+ areas measured in 4598, 2672, and 2810 islets from control aAb-, aAb+HA^{low}, and aAb+HA^{high} tissues, respectively. The values of the HA+ areas for the indicated number of islets are in ascending order. The numbers on the x-axis indicate the cumulative number of islets. (**a, b**) The cumulative numbers of islets with HA+ areas within the 500-1000 μm^2, 1001-2000 μm^2, or >2000 μm^2 size categories, presented in the light green, dark green, and red bars, respectively, (insets) are shown magnified. (**d-f**) Islet HA+ area size distribution. p<0.0005, one-way ANOVA, aAb+HA^{high} vs. control or aAb+HA^{low} tissues.

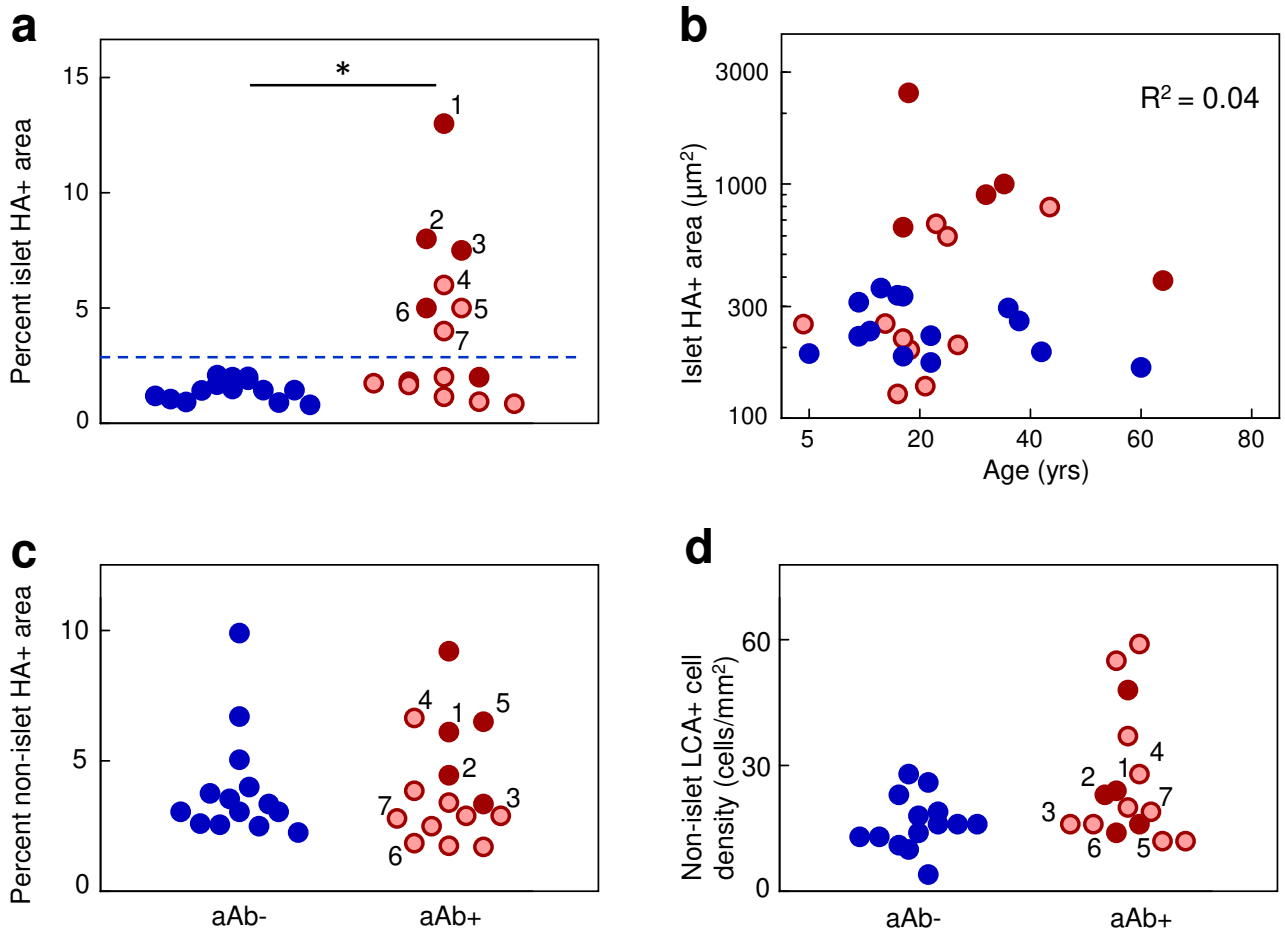

ESM Fig. 2 (**a**) Scattered plot of percent islet HA+ areas. **p*<0.0001, Mann-Whitney *U* test. The dotted line indicates the upper cut-off value (mean + 3SD) of the measurements obtained from the aAb- controls. 4598, 2672, and 2810 islets from aAb- control, aAb+HA^{low}, and aAb+HA^{high} tissues were analyzed, respectively. (**b**) Islet HA+ area as a function of donor age. Islet HA+ areas (**c**) and LCA+ cell density (**d**) in the non-islet region. Each circle denotes an individual donor. Blue circles, aAb- donors; light red circles, single aAb+; dark red circles, double aAb+.

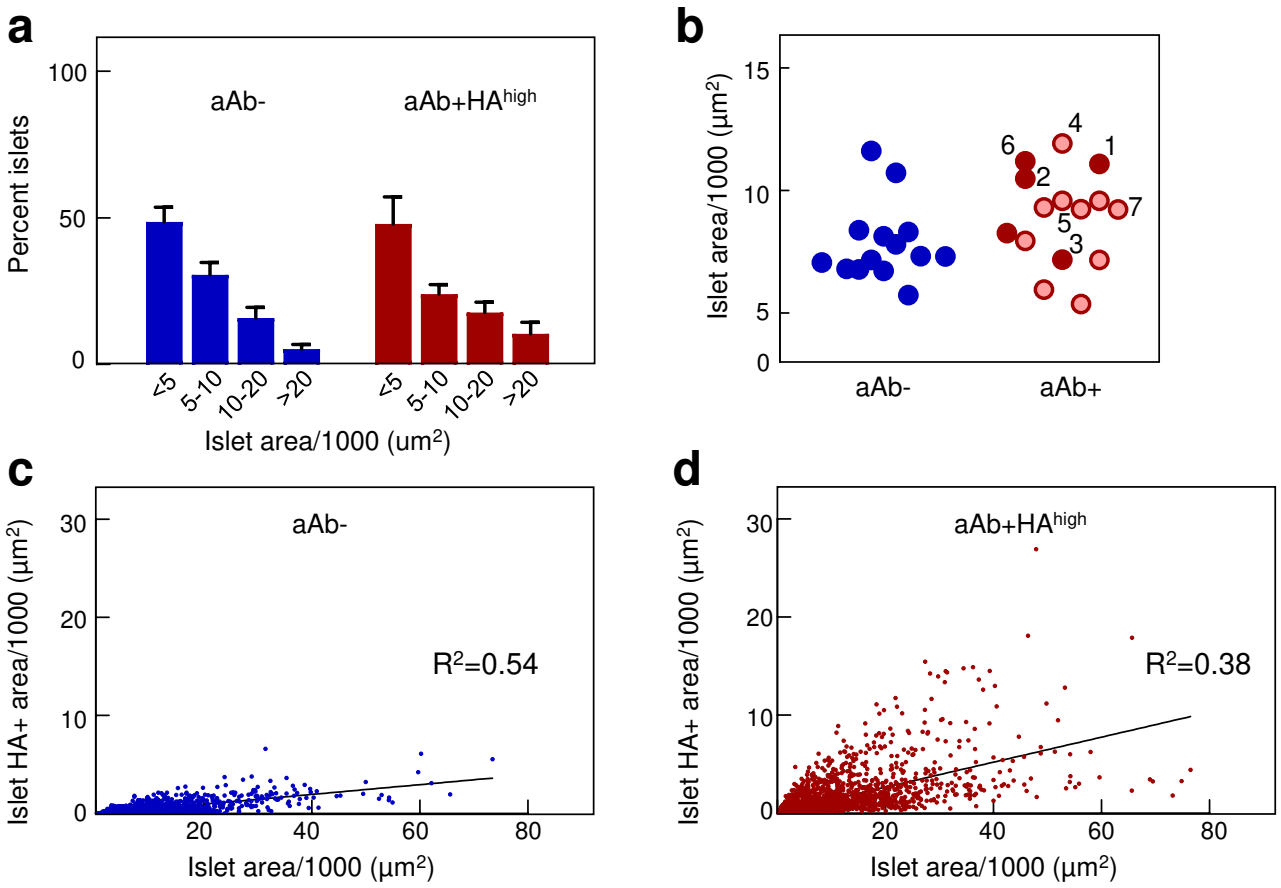

ESM Fig. 3 (**a**) Islet size distribution in 14 aAb- and 7 aAb+HA^{high} tissues. (**b**). Islet areas in each individual tissue. Islet HA+ area as a function of islet area in 14 aAb- (**c**) and 7 aAb+HA^{high} (**d**) tissues. Each circle denotes an individual donor in (b) and an individual islet in (**c** and **d**). Blue bars and circles, aAb- donors; light red circles, single aAb+; dark red bars, aAb+; dark red circles, double aAb+ in (**b**) and aAb+HA^{high} in (**d**).

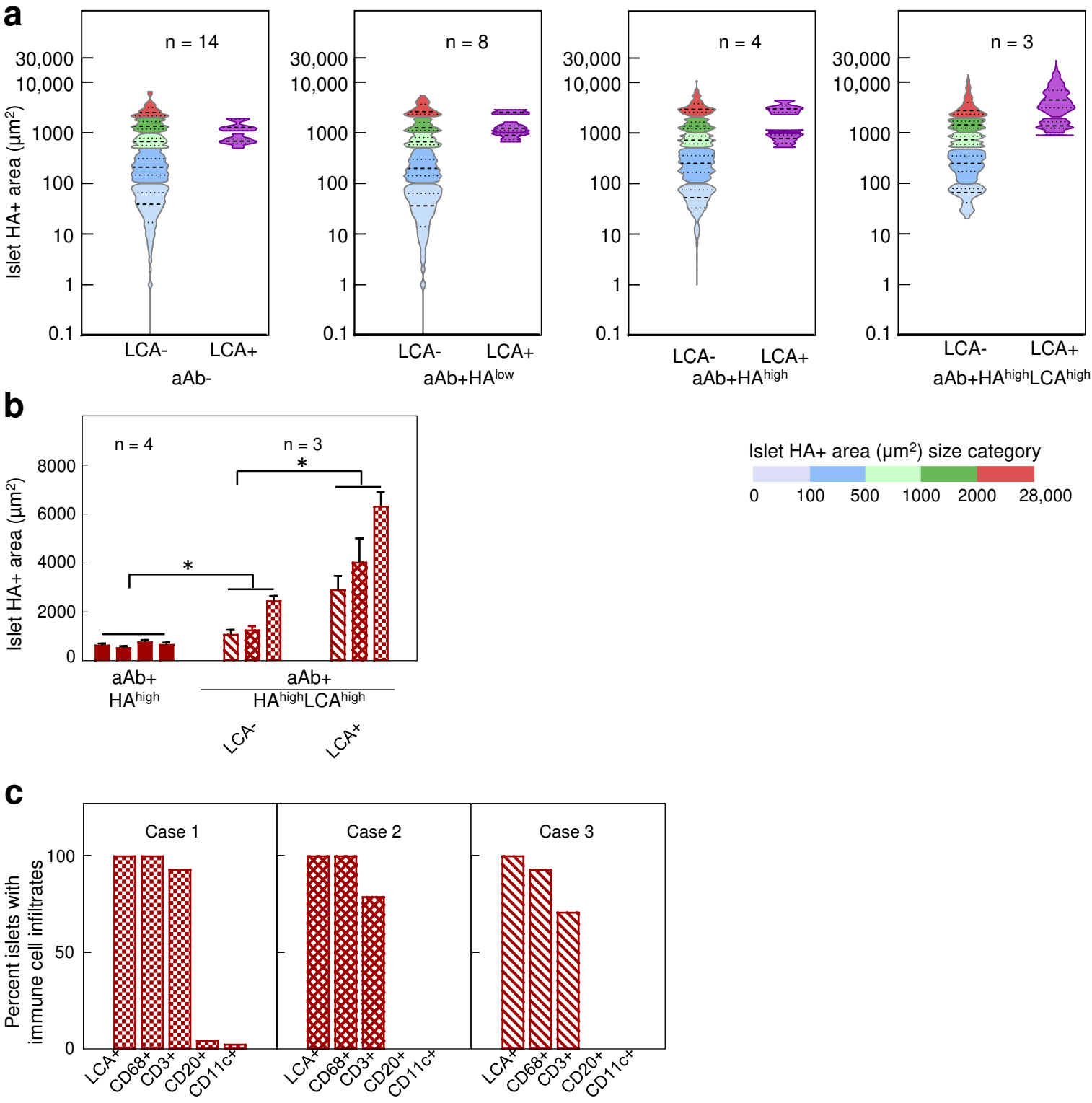

ESM Fig. 4 LCA+ leukocytes infiltrate islets exclusively in regions containing the largest HA deposits.

(**a**) Violin plots of HA+ areas in islets without (LCA-) or with (LCA+) immune cells distributed within each HA area size category. (**b**) Islet HA+ areas in the 7 individual aAb+HA^{high} tissues. Each bar represents one tissue. Solid bars, 4 aAb+HA^{high} tissues which showed no evidence of insulitis; hatched bars, 3 aAb+HA^{high} tissues with insulitis. In the 3 aAb+HA^{high}LCA^{high} tissues, immune cell-free islets (LCA-) and islets with associated immune cells (LCA+) are assessed separately. Data are mean ± SEM of the measurements. *p<0.001, Mann-Whitney U test. (**c**) Proportion of islets with LCA+ cell infiltrates containing CD68+, CD3+, CD20+, and CD11c+ cells.

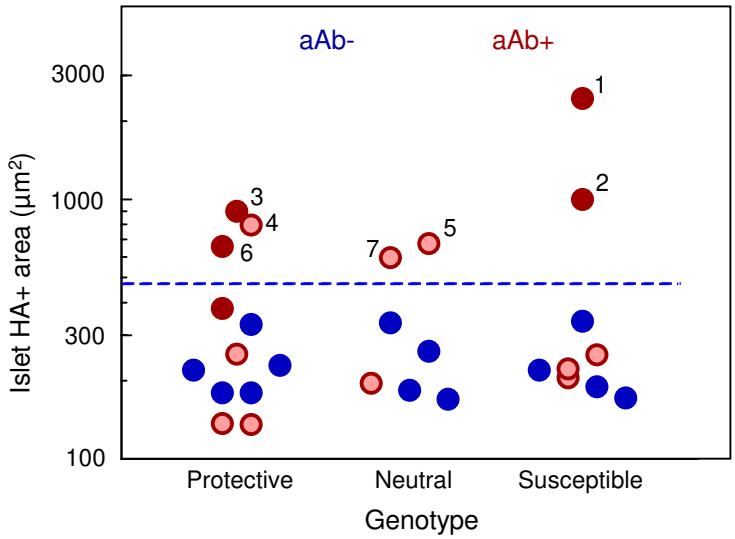

ESM Fig. 5 Scattered plot of islet HA+ areas as a function of donor HLA genotypes associated with type 1 diabetes**.** Each circle denotes an individual donor. Blue circles, aAb- donors; light red circles, single aAb+; dark red circles, double aAb+. Data are mean values of HA+ areas for each individual donor. The dotted line indicates the upper cut-off value (mean + 3SD) of the measurements obtained from the aAb- controls. The numbers 1-7 indicate the aAb+HA^{high} tissues ranked according to the size of their islet HA+ areas.

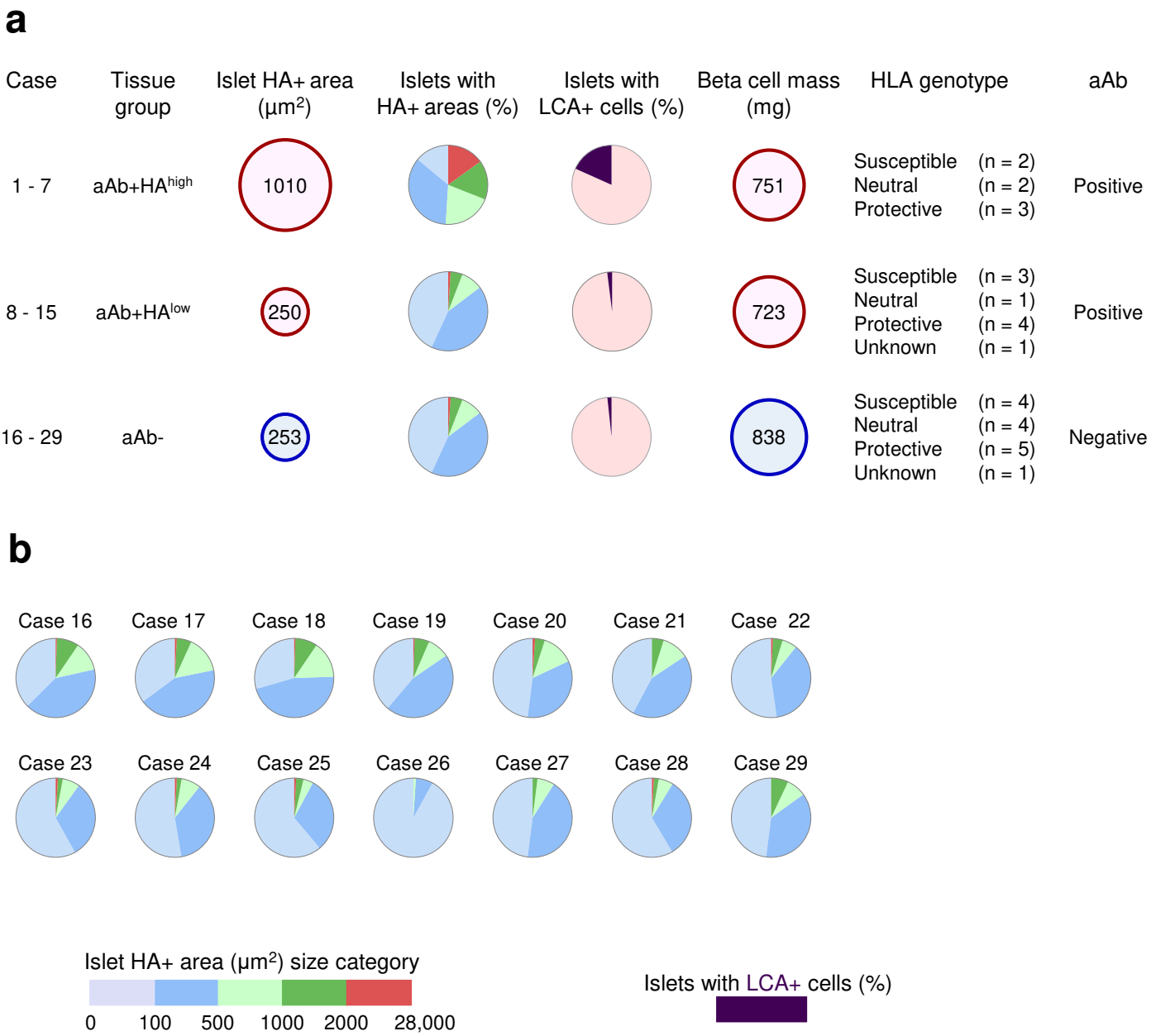

ESM Fig. 6 (**a**) Islet HA+ areas, insulitis, and beta cell mass in tissues from all donors. Data are mean values of measurements made in the 7 aAb+HA^{high}, 8 aAb+HA^{low}, and 14 control aAb- tissues. The pie charts represent the mean percentage of islets with HA+ areas falling within each of the HA+ areas size categories or the percentage of islets with LCA+ cells. The size of the red or blue circles is proportional to the average size of the islet HA+ areas or beta cell mass, which is indicated by the value number within the circle. The measurements made in islets from the individual aAb+ donors are shown in Fig. 6. In the tissues from the 14 aAb- donors: Size range of islet HA$^+$ areas, 172 to 375 µm^2; range of proportion of islets with HA+ areas, 38 to 59% for <100 µm^2, 31 to 52% for 100-500 µm^2, 3 to 13% for 500-1000 µm^2, 2 to 8% for 1000-2000 µm^2, and 0 to <1% for >2000 µm^2; range of beta cell mass, 390 mg to 1350 mg. (**b**) Islet HA+ area size distribution in the aAb- control group. The pie charts represent the percentage of islets with HA+ areas falling within each of the HA+ area size categories.

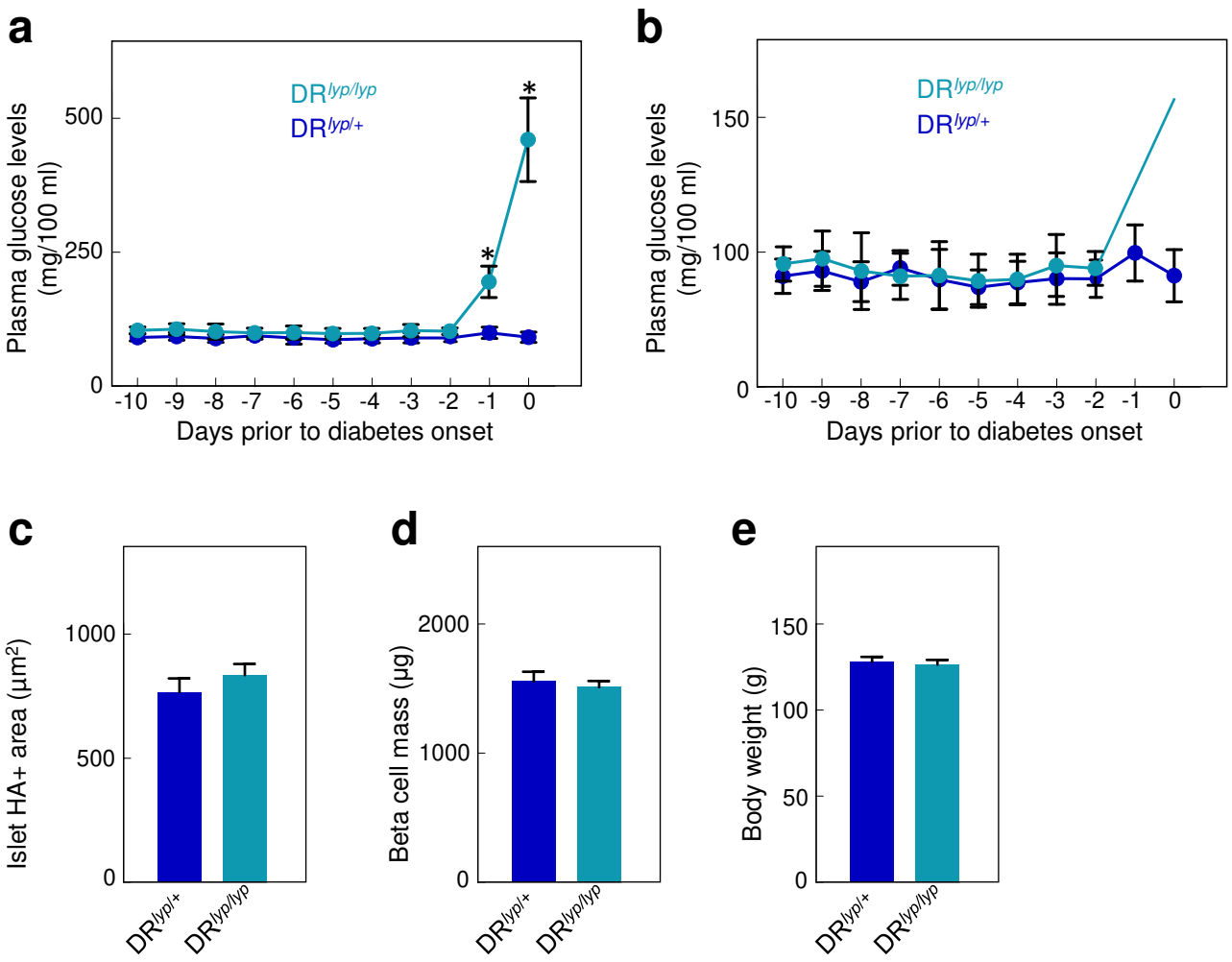

ESM Fig. 7 Assessment of morphologic and metabolic parameters in BB rats. (**a**) Fed blood glucose levels in diabetes-resistant DR$^{lyp/+}$ and diabetes-prone DR$^{lyp/lyp}$ rats. Data are mean ± SD of measurements from 10-20 rats. *p<0.001, Kruskal-Wallis test. (**b**) The blood glucose values in the two groups before the onset of hyperglycemia in the DR$^{lyp/lyp}$ rats are shown using smaller intervals on the y-axis. (**c**) Islet HA+ areas, (**d**) beta cell mass, and (**e**) body weight in DR$^{lyp/+}$ (blue bars) and DR$^{lyp/lyp}$ (light blue bars) rats at 40 days of age. Data are mean ± SD of individual measurements obtained from 20 rats in each group.

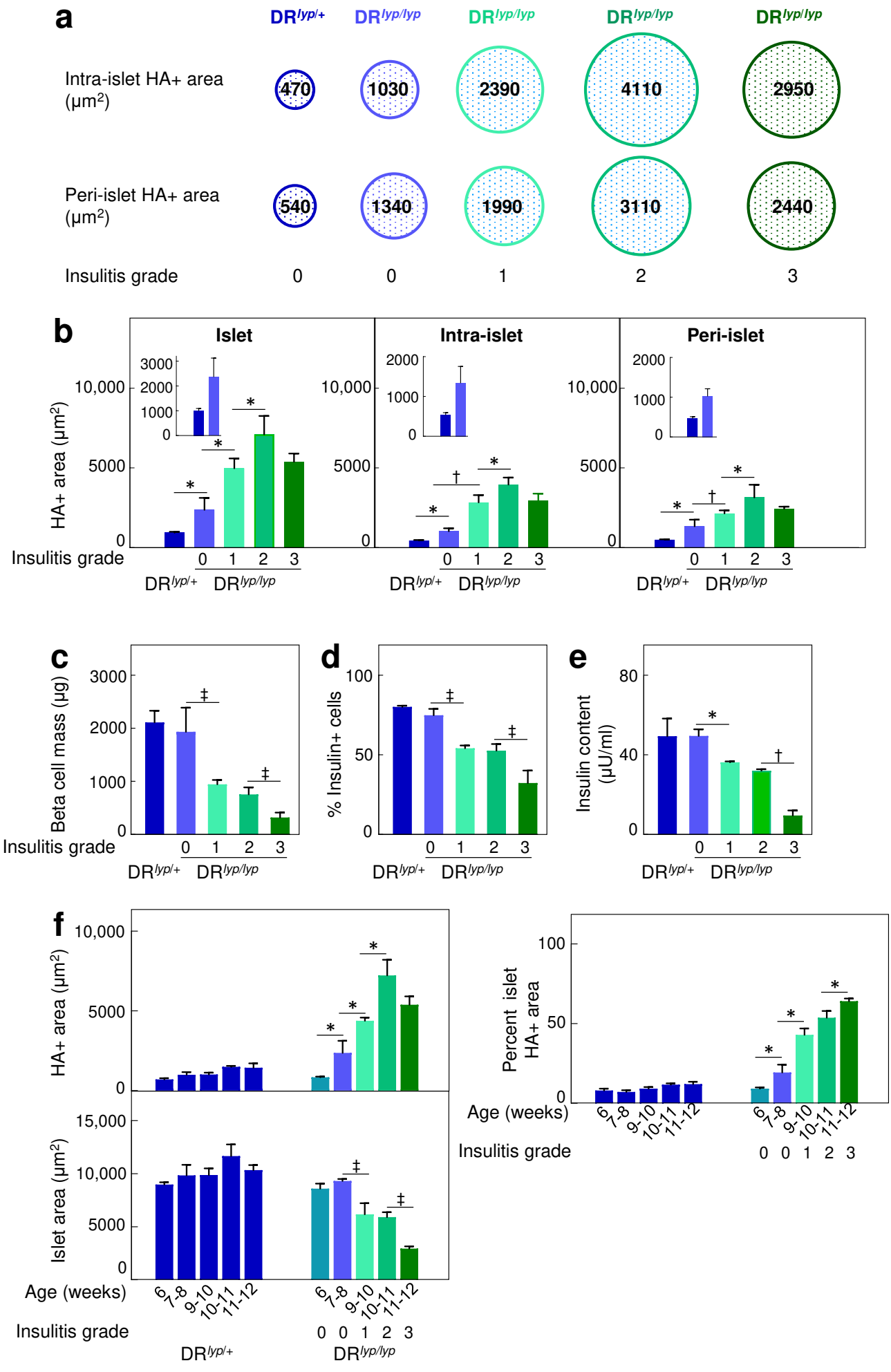
a
DR lyp/+
DR lyp/lyp
DR lyp/lyp
DR lyp/lyp
DR lyp/lyp
Intra-islet HA+ area (μm²)
470
1030
2390
4110
2950
Peri-islet HA+ area (μm²)
540
1340
1990
3110
2440
Insulitis grade
0
0
1
2
3
b
Islet
Intra-islet
Peri-islet
HA+ area (μm²)
10,000
5000
0
3000
2000
1000
2000
1000
Insulitis grade
0 1 2 3
DR lyp/+ DR lyp/lyp
c
Beta cell mass (μg)
3000
2000
1000
0
d
% Insulin+ cells
100
50
e
Insulin content (μU/ml)
80
40
f
HA+ area (μm²)
Islet area (μm²)
15,000
Percent islet HA+ area
Age (weeks)
6 7-8 9-10 10-11 11-12
0 0 1 2 3

ESM Fig. 8 HA accumulates in islets while beta cell mass decreases in presymptomatic DR$^{lyp/lyp}$ rats during the progression to hyperglycemia. (**a**) Intra- and peri-islet HA+ areas in diabetes-resistant DR$^{lyp/+}$ (blue circles) or diabetes-prone DR$^{lyp/lyp}$ (light blue and green circles) rats exhibiting different degrees of insulitis. Data are the mean values of measurements obtained from 300-400 islets (5-6 rats) per group. The size of each circle is proportional to the average size of the HA+ areas which is indicated by the value number within the circle. (**b**) Islet, intra- and peri-islet HA+ areas in tissues from DR$^{lyp/+}$ (blue bars) or DR$^{lyp/lyp}$ (light blue and green bars) rats. Left panel, data represent mean ± SEM of the measurements shown in Fig. 7k; middle and right panels, mean ± SEM of the measurements shown in (**a**) of this figure. (**c**) Beta cell mass, (**d**) percentage of insulin-positive cells, and (**e**) pancreas insulin content in DR$^{lyp/+}$ and DR$^{lyp/lyp}$ rats. (**f**) Islet HA areas and islet areas in DR$^{lyp/+}$ and DR$^{lyp/lyp}$ rats. Data are mean ± SEM of the measurements obtained from 5-6 rats per group. *p<0.05, $^{\dagger}p$<0.01, ‡ p<0.001 vs. controls, Mann-Whitney *U* test.